AFRL-AFOSR-JP-TR-2016-0086

Wave Scattering in Heterogeneous Media using the Finite Element Method

Chiruvai Vendhan
INDIAN INSTITUTE OF TECHNOLOGY MADRAS - DEPARTMENT OF OCEAN ENGINEERING

10/21/2016
Final Report

Air Force Research Laboratory
AF Office Of Scientific Research (AFOSR)/ IOA
Arlington, Virginia 22203
Air Force Materiel Command

REPORT DOCUMENTATION PAGE

Form Approved
OMB No. 0704-0188

1. REPORT DATE *(DD-MM-YYYY)*	2. REPORT TYPE	3. DATES COVERED *(From - To)*
23-10-2016	Final	22 Mar 2012 to 21 Mar 2015

4. TITLE AND SUBTITLE
Wave Scattering in Heterogeneous Media using the Finite Element Method

5a. CONTRACT NUMBER

5b. GRANT NUMBER
FA2386-12-1-4026

5c. PROGRAM ELEMENT NUMBER
61102F

6. AUTHOR(S)
Chiruvai Vendhan

5d. PROJECT NUMBER

5e. TASK NUMBER

5f. WORK UNIT NUMBER

7. PERFORMING ORGANIZATION NAME(S) AND ADDRESS(ES)
INDIAN INSTITUTE OF TECHNOLOGY MADRAS - DEPARTMENT OF OCEAN ENGINEERING
IIT MADRAS
CHNNAI, 21421016 IN

8. PERFORMING ORGANIZATION REPORT NUMBER

9. SPONSORING/MONITORING AGENCY NAME(S) AND ADDRESS(ES)
AOARD
UNIT 45002
APO AP 96338-5002

10. SPONSOR/MONITOR'S ACRONYM(S)
AFRL/AFOSR IOA

11. SPONSOR/MONITOR'S REPORT NUMBER(S)
AFRL-AFOSR-JP-TR-2016-0086

12. DISTRIBUTION/AVAILABILITY STATEMENT
A DISTRIBUTION UNLIMITED: PB Public Release

13. SUPPLEMENTARY NOTES

14. ABSTRACT
The primary aim of this study is to develop a finite element model for elastic scattering by axisymmetric bodies submerged in a heterogeneous ocean acoustic waveguide.

15. SUBJECT TERMS
Acoustics, Finite Element Methods, Wave propagation

16. SECURITY CLASSIFICATION OF:			17. LIMITATION OF ABSTRACT	18. NUMBER OF PAGES	19a. NAME OF RESPONSIBLE PERSON
a. REPORT	b. ABSTRACT	c. THIS PAGE			HONG, SENG
Unclassified	Unclassified	Unclassified	SAR	48	**19b. TELEPHONE NUMBER** *(Include area code)* 315-229-3519

Standard Form 298 (Rev. 8/98)
Prescribed by ANSI Std. Z39.18

Final Report for AOARD Grant FA 2386-12-4026

Date September 20, 2016

Title of the Project: Wave Scattering in Heterogeneous Media using the Finite Element Method

Principal Investigator : C.P. Vendhan
vendhancp@gmail.com
Institution: *Department of Ocean Engineering,*
Indian Institute of Technology Madras
Chennai, Tamilnadu 600036
India

Collaborator: Saba Mudaliar
saba.mudaliar@us.af.mil
Institution: *Sensors Directorate*
Air Force Research Laboratory
Wright-Patterson AFB, OH 45433
USA

AOARD Program Officer: Dr. Seng Hong

Period of Performance: March/22/2013 – Sept/21/2015

Abstract

Elastic scattering by structures embedded in an ocean acoustic waveguide is a problem of paramount importance. Apart from methods such as the T-matrix method, numerical methods such as the finite element method and virtual source approach have been developed to study this problem. The present study is concerned with the development of a finite element model for elastic scattering by objects in depth and range dependent ocean waveguides. The solution to the three dimensional Helmholtz equation in a cylindrical coordinate system has been expanded in a Fourier series in the azimuthal coordinate. The resulting two dimensional Helmholtz equation for each Fourier harmonic has been solved using a finite element model. The acoustic pressure field in the waveguide due to a point source insonifying an elastic object in the waveguide has been decomposed in to rigid scattering and radiation components. An assumed mode model has been chosen to formulate the radiated field due to structural vibration. The radiation loading has been identified in terms of added mass and radiation damping and the associated waveguide models have been discussed. The FE model for the waveguide requires the depth eigensolution at the truncation boundary in order to impose absorbing boundary conditions. A Rayleigh-Ritz approximation has been developed to obtain the depth eigensolution. The depth modes have a compact form consisting of a linear combination of isovelocity modes. The research work is being pursued employing the FORTAN90 code developed implementing the proposed finite element model for the waveguide scattering problem.

Chapter 1
Introduction

1.1 General

Elastic scattering by structures submerged in an ocean waveguide is a problem of paramount importance. The waveguide, by virtue of its boundaries and possible heterogeneity of the acoustic medium, would influence the elasto-acoustic behavior of the structure and far-field acoustics in the waveguide. A study of this problem requires a structural dynamic formulation, a formulation dealing with acoustic propagation in the waveguide and appropriate interface conditions at the fluid-structure/body interface. The present study is primarily concerned with waveguide acoustics, but the motivation for the study is established by considering a coupled formulation involving structural dynamic and fluid dynamic equations, which is familiarly known as the fluid-structure interaction (FSI) problem.

1.2 Literature Review

Rigid body scattering and elastic scattering from objects in an unbounded domain have been studied by analytical methods for simple geometries. Powerful numerical methods such as the transition matrix (T-matrix) method, boundary element method (BEM), and finite element method (FEM) have been developed over the years to study the scattering problem involving complex geometries. In this context, an important component of domain discretization method such as the FEM is the use of appropriate nonreflecting or absorbing boundary condition at a boundary that truncates an otherwise infinite domain. Scattering analysis of bodies in an ocean waveguide presents additional difficulties because of the sea surface and the seafloor, apart from possible stratification of acoustic properties of the medium.

In most studies, the wave-theoretical formulation has been employed assuming the waveguide to be cylindrically symmetric, which then restricts the scatterer geometry to be axisymmetric. Hackman and Sammelmann (1986) extended the T-matrix formulation to scattering in inhomogeneous waveguides. The analysis is done in two steps. The first one involves the analysis of an empty waveguide (i.e. without the scatterer in it) with a point source for which a normal mode approach has been adopted. The second problem considers the same waveguide with the scatterer located in it for which the T-matrix method has been employed. They have observed multiple scattering of acoustic waves by the scatterer and waveguide boundaries, and the inhomogeneous layers in the waveguide may be important in shallow water waveguides. They have further observed that even in long range propagation, multiple scattering effects might be important if there is appreciable sound–speed gradient in the vicinity of the scatterer.

Ingenito (1987) presented a method for scattering analysis of axisymmetric bodies in a horizontally stratified waveguide. He used the waveguide Green's functions. Thus this model fully accounts for multiple reflections at the waveguide boundaries, but it does not provide for multiple reflections

at the scatterer surface because of the use of free space scattering function. For this reason, this model is called a *single-scatter model.* Ingenito (1987) presented results for a spherical scatterer and outlined the formulation for a non-spherical body. He has noted that the method may fail for depth-dependent sound speed profiles because of the presence of evanescent modes.

Hackman and Sammelmann (1988) presented multiple scattering analysis for a target in a waveguide. Unlike Ingenito (1987), these authors have used free-space Green's functions. They have noted that rescattering from the object/target located in a shallow water waveguide could be important if there is significant amount of radiation from it in the vertical direction.

Collins and Werby (1988) presented a simple and efficient method using the parabolic equation model for scattering in a range-dependent waveguide.

Norman and Werby (1991) presented a T-matrix model, which implies a single scatter approximation similar to Ingenito. They have shown through examples that the scattering object is correctly coupled to the waveguide. *An object is said to be correctly coupled to the waveguide if the scattered field displays the same characteristics as the field produced by a point source.*

Perkins *et al.* (1992) extended Ingenito's modal approach to weakly range-dependent problems using the adiabatic approximation.

Makris (1998) presented a spectral formulation for studying the scattering characteristics of a non-compact (i.e., $1 < ka$, the scattering parameter) object in a shallow water waveguide, by generalizing the single-scatter modal approach of Ingenito.

The foregoing works employ one or more of the following restrictions to facilitate the scattering formulation: i) the waveguide is range-independent or at best weakly range dependent and ii) single-scattering which ignores multiple scattering from the object; iii) The object is far removed from the boundaries of the waveguide so that free space scattering functions of the object can be used; and iv) the object is sufficiently far from the source and the receiver. The coupled mode method of Evans (1983), and full-fledged numerical methods such as the FEM and virtual source approach (VSA) can handle the general case of scattering in range-dependent waveguides. Zampolli et al. (2007) developed a finite element model for scattering by an axisymmetric structure immersed in a range and depth dependent cylindrically symmetric waveguide. They employed perfectly matched layers (PML) at the truncation boundaries to simulate absorbing boundary conditions. In the VSA, which has been briefly reviewed in Jensen et al (2011) with key references, several point sources of unknown intensity are distributed over the scatterer and the source intensities are obtained by solving a set of global equations. The main thrust of the present study is to formulate a 3-D finite element model for range and depth dependent cylindrically symmetric waveguides with axisymmetric objects embedded in them.

1.3 Aim and Scope of the Study

The primary aim of this study is to develop a finite element model for elastic scattering by axisymmetric bodies submerged in a heterogeneous ocean acoustic waveguide. A 3-D formulation for nonaxisymmetric scattering and radiation in a cylindrically symmetric waveguide is considered wherein the azimuthal variation in the acoustic field is represented using a Fourier series and the Helmholtz equation for each of the harmonics is solved using a finite element model. As a part of the present work, a Rayleigh-Ritz approximation for the depth eigenproblem has been developed. The depth eigensolution obtained using this model has been employed at the truncation boundary of the FE model for the waveguide.

For convenience, the elastic scattering problem is decomposed into rigid scattering and radiation problems. In order to bring out the relevance of waveguide radiation analysis, a compact dynamic model for a structure vibrating in contact with a fluid is discussed in Chapter 2. 3-D acoustic waveguide propagation models corresponding to incident wave, scattering and radiation problems are discussed in Chapter 3. A finite element model for solving a typical waveguide problem is presented in Chapter 4. A Rayleigh-Ritz approximation is presented for the solution of the depth eigenproblem in Chapter 5. The eigensolution, which is in a compact form, has been used in the finite element model. Salient observations are made in Chapter 6.

Chapter 2
Acoustic Radiation Loading on Structures Immersed in an Ocean Acoustic Waveguide

2.1 Introduction

Fluid-structure interaction (FSI) formulations involving vibrations of structures, such as plate and shell structures, in contact with a fluid are coupled in nature. A typical FSI formulation involves structural dynamic and fluid dynamic equations, which, by virtue of coupling between them, have mutual influence. In this context, the acoustic fluid model (i.e., a compressible inviscid fluid model, Junger and Feit; 1972) is considered adequate, although viscous compressible fluid models are now feasible with the emergence of powerful CFD codes, but such an option would be computationally voluminous. FSI problems are generally solved using numerical methods such as the BEM and FEM. A compact analysis technique for relatively simple FSI problems consists of the use of an assumed mode expansion for the structural displacements within the framework of a variational formulation, which results in a set of coupled discrete equations in the time domain. Time harmonic FSI problems have an interesting feature namely, the hydrodynamic/acoustic problem can be solved first for each of the assumed modes having unit amplitude (Junger and Feit, 1972). The results of the acoustic problem can then be incorporated in the structural dynamic equations in the form of modal fluid loads with unknown amplitudes. The solution of the structural dynamic equation at this stage essentially solves the problem *fully*, i.e., both the structural and fluid response quantities are determined at this stage. This approach may be looked upon as a sequential analysis procedure applied to an otherwise coupled problem which results in great computational economy. Such an approach is also widely employed in the study of rigid body motions of floating systems such as ships subjected to small amplitude monochromatic water waves.

A brief outline of the FSI formulation is first presented and then specialized to the case of harmonic response, in the following sections. The fluid loading on the structure due to its motion may be obtained by solving the acoustic waveguide propagation problem, for a set of assumed modes of unit amplitude. The fluid loading is often referred to as the acoustic radiation loading. *This provides the motivation for the study of acoustic radiation from bodies located in an ocean waveguide.*

2.2 Formulation of FSI Problems

Consider small amplitude, elastic vibrations of a shell in contact with an acoustic fluid. Let $\left\{\hat{\bar{u}}\right\} = \left\langle \hat{u}, \hat{v}, \hat{w} \right\rangle^T$ denote the time-dependent meridional, circumferential and radial displacements of the shell. Let the generalized strain array be denoted by $\left\{\varepsilon\right\}$ and the corresponding (symmetric) elasticity matrix by $\left[D\right]$. The strain array may be related to the displacement vector as

$$\{\varepsilon\} = [L]\{\hat{\bar{u}}\} \tag{2.1}$$

where the operator matrix $[L]$, which denotes the generalized strain-displacement relation, may readily be identified from the shell theory adopted (see Junger and Feit, 1972). Then, the strain energy of the shell is given by

$$\bar{U} = \frac{1}{2}\int_S \{\varepsilon\}^T [D]\{\varepsilon\}\, dS \tag{2.2}$$

where *S* denotes the surface of the shell. The kinetic energy may be written, after neglecting the rotary inertia contribution, as

$$T = \frac{1}{2}\int_S m \begin{Bmatrix} \dot{\hat{u}} \\ \dot{\hat{v}} \\ \dot{\hat{w}} \end{Bmatrix}^T \begin{Bmatrix} \dot{\hat{u}} \\ \dot{\hat{v}} \\ \dot{\hat{w}} \end{Bmatrix} dS \tag{2.3}$$

where *m* denotes the mass per unit surface area of the shell and a (.) indicates differentiation with respect to time *t*.

As an approximation, let the displacement field be expressed as a linear combination of a number of *appropriate* assumed modes, say $U_1, U_2, \ldots, U_{n1}$, for $\hat{u}$, $V_1, V_2, \ldots, V_{n2}$, for $\hat{v}$, and $W_1, W_2, \ldots, W_{n3}$, for $\hat{w}$, all being functions of the spatial variables only. Then, the displacement components may be written as

$$\{\hat{\bar{u}}\} \approx \begin{Bmatrix} \hat{u} \\ \hat{v} \\ \hat{w} \end{Bmatrix} = \begin{bmatrix} U_1, U_2, \ldots U_{n1}, 0, 0, \ldots & \\ 0, 0, \ldots & , V_1, V_2, \ldots V_{n2}, 0, 0, \ldots \\ 0, 0, \ldots & 0, 0, \ldots W_1, W_2, \ldots W_{n3} \end{bmatrix} \langle \hat{a}_1, \hat{a}_2, \ldots \hat{a}_{n1}, \hat{b}_1, \hat{b}_2, \ldots, \hat{b}_{n2}, \hat{c}_1, \hat{c}_2, \ldots, \hat{c}_{n3} \rangle^T \tag{2.4a}$$

or

$$\{\hat{\bar{u}}\} = [N]\{\hat{d}\} \tag{2.4b}$$

where $\hat{d}_j(t), j = 1,2,\ldots(n_1 + n_2 + n_3)$ denote the unknown generalized coordinates which are functions of time *t*. For convenience, define an array $\{\bar{N}\}$ such that

$$\{\bar{N}\}^T = \langle U_1, U_2, \ldots U_{n1}, V_1, V_2, \ldots V_{n2}, W_1, W_2, \ldots W_{n3} \rangle \tag{2.4c}$$

which will be used later. In the view of Eq. (2.4b), the strain array in Eq. (2.1) may be written as

$$\{\varepsilon\} = [L][N]\{\hat{d}\} = [B]\{\hat{d}\} \tag{2.5}$$

In view of Eq. (2.5), the strain energy and kinetic energy of the shell respectively in Eqs. (2.2) and 2.3 may be written as

$$\bar{U} = \frac{1}{2}\int_S \left\{\hat{d}\right\}^T [B]^T [D][B]\left\{\hat{d}\right\} dS \tag{2.6}$$

$$T = \frac{1}{2}\int_S m\left\{\dot{\hat{d}}\right\}^T [N]^T [N]\left\{\dot{\hat{d}}\right\} dS \tag{2.7}$$

Let the excitation/dynamic load, including fluid dynamic loading at the fluid-solid interface, acting on the structure be denoted as

$$\left\{\hat{f}\right\} = \left\langle \hat{f}_u, \hat{f}_v, \hat{f}_w \right\rangle^T \tag{2.8}$$

where the three components on the r.h.s. correspond to the three coordinate directions. The virtual work done by the dynamic load may be written as

$$\delta W(t) = \int_S \left\{\delta\hat{\bar{u}}\right\}^T \left\{\hat{f}\right\} dS = \int_S \left\{\delta\hat{d}\right\}^T [N]^T \left\{\hat{f}\right\} dS \tag{2.9a}$$

or, using the notation in Eq. (2.4c),

$$\delta W = \sum_{j=1}^{n_1}\int_S \hat{f}_u \bar{N}_j \delta\hat{d}_j dS + \sum_{j=n_1+1}^{n_1+n_2}\int_S \hat{f}_v \bar{N}_j \delta\hat{d}_j dS + \sum_{j=n_1+n_2+1}^{n_1+n_2+n_3}\int_S \hat{f}_w \bar{N}_j \delta\hat{d}_j dS \tag{2.9b}$$

which may be written symbolically as

$$\delta W = \sum_{j=1}^{n_1+n_2+n_3} \hat{Q}_j(t)\,\delta\hat{d}_j \tag{2.9c}$$

where $\hat{Q}_j(t)$ denotes the generalized load associated with $\hat{d}_j$. The fluid dynamic loading, which is part of the generalized load, will be discussed in Sec. 2.3 dealing with harmonic response.

The Lagrange equations of motion of the shell may be written, using Eqs. (2.6), (2.7) and (2.9), as

$$\frac{d}{dt}\left(\frac{\partial T}{\partial \dot{\hat{d}}_j}\right) - \left(\frac{\partial \bar{U}}{\partial \hat{d}_j}\right) = \hat{Q}_j \tag{2.10}$$

Upon using the expressions for K.E. and P.E. given in Eqs. (2.6) and (2.7), the matrix equation of motion is obtained from Eq. (2.10) as,

$$[M]\left\{\ddot{\hat{d}}\right\} + [K]\left\{\hat{d}\right\} = \left\{\hat{Q}\right\} \tag{2.11}$$

where the symmetric stiffness matrix is given by

$$[K] = \int_S [B]^T [D][B] dS \tag{2.12a}$$

and the symmetric mass matrix is given by

$$[M] = \int_S m[N]^T [N] dS \tag{2.12b}$$

Note that Eqs. (2.12a) and (2.12b) are valid for time-invariant heterogeneous elastic and mass properties. The surface integrals above may in general be evaluated using numerical quadrature.

It may be noted that the generalized fluid load component in $\left\{\hat{Q}\right\}$ (see Eq. (2.11)) is unknown, which can only be obtained by solving the fluid dynamic equation. But such a solution requires constraints imposed by the fluid on structural motion at the fluid-solid interface which is also unknown. Thus, the structural dynamic equations in (2.11) and the fluid dynamic equations for the waveguide (discussed in Chapter 3) are coupled, which is characteristic of typical FSI problems.

2.3 Response to Harmonic Excitation

Let the harmonic excitation with circular frequency ω be given in the form

$$\left\{\hat{f}(t)\right\} = \left(\left\{f_E\right\} + \left\{f_p\right\}\right) exp\left(-i\omega t\right) \tag{2.13}$$

where $\left\{f_E\right\}$ denotes a known excitation amplitude which may be acoustic (say, due to flow noise) or non-acoustic in origin, and $\left\{f_p\right\}$ the excitation amplitude associated with the scattered and radiated acoustic fields for elastic scattering problems. Since the problem under study is linear, the structural response to harmonic excitation may be written as

$$\left\{\hat{d}\right\} = \left\{d\right\} exp\left(-i\omega t\right) \tag{2.14a}$$

The acoustic pressure field in the fluid domain would also be harmonic, which may be written, using linear superposition, as

$$\hat{p}(t) = \left(p_{Rs} + p_{Rad}\right) exp\left(-i\omega t\right) \tag{2.14b}$$

Here, p_{Rs} denotes the total complex pressure on the surface of the body resulting from rigid scattering of the incident field by the body located in the waveguide, which of course is obtained by assuming the body to be rigid. This involves solving a rigid scattering problem in the waveguide, which is discussed in Chapter 3. Similarly, p_{Rad} denotes the complex pressure on the body surface due to the radiated field, which is caused by *structural motion in the radial direction only, since the fluid has been assumed to be inviscid.* For the same reason, acoustic/hydrodynamic pressure p is the only load acting on the structure at the fluid-solid interface as a result of FSI. So, in view of Eq. (2.9c), the virtual work done by these pressure forces may be written as

$$\delta W_p = \left(\sum_{j=(n_1+n_2+1)}^{n_1+n_2+n_3} Q_{pj}\delta d_j\right) exp\left(-2i\omega t\right) \tag{2.15}$$

where, using Eq. (2.9b), the generalized complex pressure force may be written, using the notation in Eq. (2.4c), as

$$\begin{aligned} Q_{pj} &= -\int_S \left(p_{Rs} + p_{Rad}\right)\bar{N}_j dS \qquad j = \left(n_1+n_2+1\right),\left(n_1+n_2+2\right),.....\left(n_1+n_2+n_3\right) \\ &= 0 \qquad\qquad\qquad\qquad\qquad\qquad \text{othewise} \end{aligned} \tag{2.16}$$

where the negative sign indicates the pressure is directed opposite to the outward normal of the structural surface. Using the above, the harmonic response equation for the structure may be written, in view of Eq. (2.11) as

$$\left(-\omega^2[M]+[K]\right)\{d\}=\{Q_p\}+\{Q_E\} \tag{2.17}$$

where $\{Q_p\}$ denotes the generalized pressure load due to the rigid scattering and radiation pressure acting on the body surface (see Eq. (2.14b)), which will be dealt with in Chapter 3, and $\{Q_E\}$ the generalized load due to external load on the structure.

2.4 Acoustic Radiation Loading

Consider the radiated pressure p_{Rad} in Eq. (2.16) which is obtained as a linear combination of complex radiated field p_{Rk} due to each of the assumed radial modes, say W_k in Eq. (2.4a). This involves solving a waveguide propagation problem, in which the body is located in the waveguide and the normal derivative of pressure corresponding to *k*-th radial mode W_k is imposed at the fluid-body interface. Note that this condition ensures velocity matching at the interface. The above boundary condition for the acoustic problem may be written in general as

$$\frac{\partial \hat{p}_{Rk}}{\partial n}=-\rho\frac{\partial^2 \hat{w}_k}{\partial t^2} \tag{2.18}$$

where *n* denotes the normal outward of the fluid domain, ρ the density of the fluid and the harmonic radial displacement is given by

$$\hat{w}_k = W_k\, exp\left(-i\omega t\right) \tag{2.19a}$$

Then, for the time-harmonic case, considering the *k*-th radial mode mentioned above, in view of Eq. (2.4a), Eq. (2.18) reduces as

$$\frac{\partial p_{Rk}}{\partial n}=\rho\omega^2 W_k d_k \tag{2.19b}$$

It is convenient to solve the waveguide problem with unit amplitude of $\frac{\partial p}{\partial n}$ as W_k at the body-fluid interface. Denoting the radiated pressure in this case by p_{Rk0}, the actual radiated field due to the *k*-th mode may be written, including the modal coefficient d_k, as

$$p_{Rk}=\rho\omega^2 p_{Rk0} d_k \tag{2.20}$$

Then, in view of Eq. (2.16), the generalized radiated pressure load, with all the assumed modes included, may be written as

$$Q_{pj}=\int_S \sum_{k=n_1+n_2+1}^{n_1+n_2+n_3} p_{Rk}\bar{N}_j dS \qquad j=n_1+n_2+1, n_1+n_2+2,\ldots n_1+n_2+n_3 \tag{2.21a}$$

or

$$Q_{pj} = \sum_{k=n_1+n_2+1}^{n_1+n_2+n_3} F_{jk} d_k \tag{2.21b}$$

Added mass and radiation damping

The complex loading in Eq. (2.21) can be decomposed in to inertia and damping load components. The inertia load component may be written, for harmonic case, as

$$-[A]\left\{\ddot{\hat{d}}\right\} = \omega^2 [A]\{d\} exp(-i\omega t)$$

where the negative sign is based on D'Alembert's principle. Here $[A]$ has the unit of mass, and hence it is called the *Added Mass matrix*, which again is real valued.

The damping load may be written, for the harmonic case, as

$$[B]\left\{\dot{\hat{d}}\right\} = -i\omega[B]\{d\} exp(-i\omega t)$$

where $[B]$ has the unit of damping constant, and hence called the *Radiation Damping Matrix*, which is again real valued. Note that both $[A]$and $[B]$ are symmetric and frequency dependent.

Thus, the complex generalized pressure amplitude in Eq. (2.21b) may be written as

$$F_{jk} = \omega^2 \left[A(\omega)\right] - i\omega\left[B(\omega)\right] \tag{2.22}$$

where,

$$A_{jk} = \frac{1}{\omega^2}\mathrm{Re}\left(F_{jk}\right) \;\; ; \;\; B_{jk} = -\frac{1}{\omega}\mathrm{Im}\left(F_{jk}\right) \tag{2.23a}$$

with $Re(\cdot)$ and $Im(\cdot)$ denoting respectively the real and imaginary parts. In actual computation, the factor $\rho\omega^2$ need not be used as in Eq. (2.20), and hence evaluate the integral in Eq. (2.21a) using p_{Rk0} to obtain F'_{jk} .Then Eq. (2.23a) may be written as

$$A_{jk} = \rho\mathrm{Re}\left(F'_{jk}\right) \;\; ; \;\; B_{jk} = -\rho\omega\,\mathrm{Im}\left(F'_{jk}\right) \tag{2.23b}$$

The primary goal of waveguide analysis, with the radiating body included in the fluid domain (which is discussed in Chapter 3), is to evaluate added mass and damping parameters.
In view of Eqs. (2.22) and (2.23), the harmonic response equation in (2.17) may be written as,

$$\left(-\omega^2\left([M]+\left[\overline{A}\right]\right) - i\omega\left[\overline{B}\right] + [K]\right)\{d\} = \{Q'\} \tag{2.24}$$

where $\{Q'\}$ denotes generalized loads due to scattered pressure and due to any source of excitation, as mentioned under Eq. (2.13). The inviscid fluid model used does not obviously give rise to any tangential fluid dynamic loading on the body fluid interface although the structural motion considered involves both radial and tangential components (see section 2.2). So the added mass and radiation damping matrices in Eq. (2.24) may be written as

$$\left[\bar{A}\right]=\begin{bmatrix}0, & 0\\ 0, & [A]\end{bmatrix}, \left[\bar{B}\right]=\begin{bmatrix}0, & 0\\ 0, & [B]\end{bmatrix} \tag{2.25}$$

where the trivial entries correspond to the tangential displacement variables. It may be observed that since the acoustic radiation loading in Eq. (2.22) depends on structural motion, its effect has been appended to the structural mass and stiffness terms as seen in Eq. (2.24). Solution of Eq. (2.24) yields the structural harmonic motion amplitude array $\{d\}$ associated with the assumed modes in Eq. (2.4a). Having obtained the structural response values, the radiated field in the waveguide can readily be quantified using Eq. (2.20).

2.5 Conclusion

The structural dynamic model discussed in Sec. 2.2 is a classical form which is especially suited for axisymmetric structures, and it results in a compact dynamic model. The azimuthal/ circumferential modes would obviously be Fourier harmonics. Legendre functions should provide a convenient choice for the meridional modes. It might be noted that the assumed modes approach discussed above would readily handle mass and stiffness variations in axisymmetric shells, as indicated under Eq. (2.12). If it is desired to employ FE models for complex axisymmetric shell structures, the dry modeshapes may first be derived from a FE model. Then, it would be convenient to obtain a least squares fit to these meridional modeshapes using assumed modes in the form of Legendre functions and then employ the formulation outlined in the foregoing sections.

Chapter 3
Formulation of Acoustic Scattering and Radiation Problems in 3-D Waveguides

3.1 Introduction

The propagation of sound waves in a medium may be analyzed using the acoustic fluid model, in which the fluid is considered inviscid but compressible. The governing equation for an ocean acoustic waveguide (OAWG) turns out to be the wave equation in terms of scalar pressure, velocity or displacement potential (Jensen et al., 2011). The wave theoretical model can handle heterogeneous acoustic properties, backscatter caused by obstructions etc. It can be generalized to include attenuation by defining a complex sound speed. Two dimensional propagation in a cylindrically symmetric waveguide is the commonly used model in ocean acoustics. A simplified model for three dimensional propagation is often constructed by considering such 2D models at a set of discrete azimuthal angles and then combining the various 2D results. Such a model obviously does not account for azimuthal/horizontal refraction/diffraction. Three dimensional propagation arises in OAWG due to factors such as azimuthal bathymetric variations, and scattering from objects in the waveguide.

In this chapter, the three-dimensional (3-D) Helmholtz equation governing the acoustic field in a cylindrically symmetric waveguide is presented. The acoustic field is expressed in a Fourier series in the circumferential/azimuthal coordinates and the governing equation reduced to a 2-D Helmholtz equation for each of the circumferential harmonics. The axisymmetric fluid domain is truncated at a radial boundary in the far field, for the purpose of FE modeling. Hence, special attention is focused on suitable absorbing boundary conditions on the truncation boundary instead of using the classical Sommerfield radiation condition, which is a limiting condition.

3.2 Mathematical Model

The fluid domain Ω defined in the cylindrical coordinate system (r,θ,z) constitutes an ocean acoustic waveguide, shown schematically in Fig. 3.1, where *z* denotes the vertical coordinate, r the radial/range co-ordinate and θ the circumferential/azimuthal coordinate.

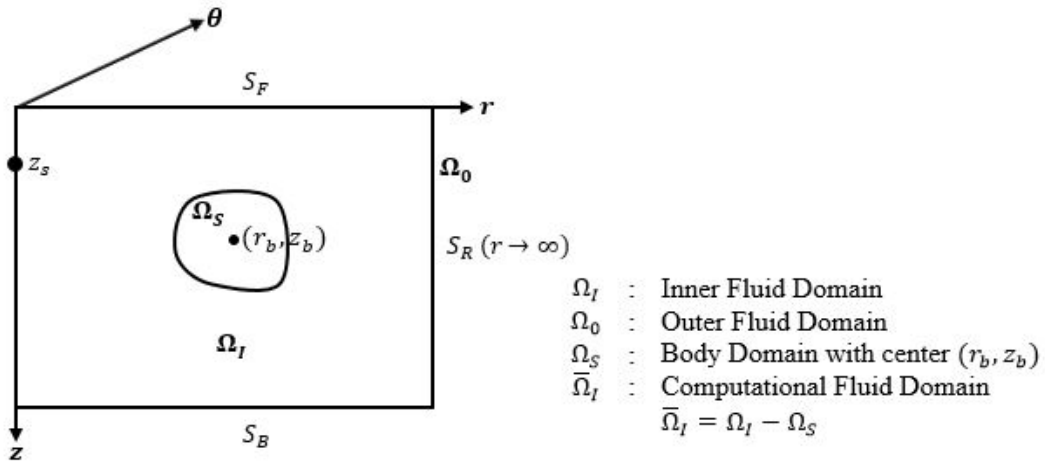

Fig. 3.1 Schematic diagram for a 3-D ocean acoustic waveguide

The waveguide, unbounded in range *r*, is bounded at the top by the plane $z = 0$, which is the air-sea interface or free surface of the ocean (S_F) and at the bottom by the seabed of arbitrary topography (S_B). An elastic scatterer, whose surface S_{IF} is in contact with the fluid, is submerged in the waveguide. The wave equation for the heterogeneous waveguide may be written in cylindrical co-ordinates as (Jensen et al., 2011),

$$\rho(r,z,\theta)\nabla.\left[\frac{1}{\rho(r,z,\theta)}\nabla\hat{p}(r,z,\theta,t)\right]+\frac{1}{c^2(r,z,\theta)}\frac{\partial^2\hat{p}(r,z,\theta,t)}{\partial t^2}=0 \tag{3.1}$$

where $\hat{p}$ denotes the time dependent acoustic pressure, ρ the density of the medium and *c* the sound speed. The gradient operator in cylindrical coordinates is given as

$$\nabla=\left\langle\frac{\partial}{\partial r},\frac{1}{r}\frac{\partial}{\partial\theta},\frac{\partial}{\partial z}\right\rangle \tag{3.2}$$

Assuming time-harmonic motion in the form $\hat{p}(r,z,\theta,t)=p(r,z,\theta)e^{-i\omega t}$, where ω denotes the circular frequency and p the 3-D complex acoustic pressure, the 3-D Helmholtz equation follows from Eq. (3.1) as

$$\rho(r,z,\theta)\nabla.\left[\frac{1}{\rho(r,z,\theta)}\nabla p(r,z,\theta)\right]+\frac{\omega^2}{c^2(r,z,\theta)}p(r,z,\theta)=0 \tag{3.3}$$

Eq. (3.3) may be expanded as

$$\rho\frac{1}{r}\frac{\partial}{\partial r}\left(\frac{1}{\rho}r\frac{\partial p}{\partial r}\right)+\rho\frac{1}{r^2}\frac{\partial}{\partial\theta}\left(\frac{1}{\rho}\frac{\partial p}{\partial\theta}\right)+\rho\frac{\partial}{\partial z}\left(\frac{1}{\rho}\frac{\partial p}{\partial z}\right)+\frac{\omega^2}{c^2}p=0 \tag{3.4}$$

Let the solution in the circumferential coordinate be written in a Fourier series. Thus, the total field may be written as,

$$p(r,z,\theta)=\sum_{m=-\infty}^{\infty}p_m(r,z)\exp(im\theta) \tag{3.5}$$

Further, it is assumed that ρ and c are independent of θ. This implies that θ – dependence of the acoustic field is entirely due to directional sources, scatterers, and radiators which are located in the waveguide.

It is important to recall that the scatterer/radiator has been assumed to be axisymmetric. Then, in view of Eq. (3.5), Eq. 3.4 may be written for the *m*-th harmonic in a decoupled form as

$$\rho(r,z)\frac{1}{r}\frac{\partial}{\partial r}\left(\frac{1}{\rho}r\frac{\partial p_m}{\partial r}\right)+\rho(r,z)\frac{\partial}{\partial z}\left(\frac{1}{\rho}\frac{\partial p_m}{\partial z}\right)+\left(\frac{\omega^2}{c^2(r,z)}-\frac{m^2}{r^2}\right)p_m=0 \tag{3.6}$$

The BVP in Eq. (3.6) should satisfy appropriate B.C. on the waveguide boundaries at $z=0$ and $z=D$. A prescribed Neumann B.C. on the boundary S_N may be written as

$$\frac{\partial p_m}{\partial n}=p_{mv} \text{ on } S \tag{3.7a}$$

where p_{mv} denotes a prescribed normal derivative of pressure. The rigid seafloor and body-fluid interface S_{IF}, which are discussed later in this section, would fall under this category.

Alternatively, a prescribed Dirichlet B.C. on the boundary S_D may be written as

$$p_m = p_{m0} \text{ on } S_D \tag{3.7b}$$

For pressure release surface such as the air-sea interface S_F, $p_{m0}=0$.

The condition on an impedance boundary S_I may be written as

$$\frac{\partial p_m}{\partial n}+ap_m=0 \text{ on } S_I \tag{3.7c}$$

where *a* denotes the surface impedance coefficient.

Apart from the above conditions, the solution to the waveguide problem should also satisfy a suitable radiation boundary condition, which is discussed in Sec. 4.3. Eqs. (3.6) and (3.7) may be adopted to study a variety of waveguide scattering problems, as discussed below. Consider an axisymmetric body (with a vertical axis as its axis of revolution) located in a cylindrical waveguide whose reference point is at (r_B, z_B) (see Fig. 3.1).

The acoustic field in the waveguide due to a point source will be scattered by this body, henceforth called the scatterer. If the scatterer is deformable, invoking linear superposition, it is convenient to consider the following decomposition (see Eq. (2.14b)) to solve this problem:

$$p=\left(p_{Rs}+p_{Rad}\right) \tag{3.8a}$$

where p_{Rs} denotes the complex rigid scattering pressure, p_{Rad} the complex radiated pressure owing to the deformability of body. It is convenient to decompose the rigid scattering pressure as a sum of the incident pressure field p_I and pressure field p_{Rs0} due scattered waves as,

$$p_{Rs}=\left(p_I+p_{Rs0}\right) \tag{3.8b}$$

Note that the decompositions in Eq. (3.8) lead to great computational convenience, and also provide an insight into elastic scattering phenomenon. The incident pressure in Eq. (3.8b) indeed denotes the acoustic field caused by a source in an 'empty waveguide', i.e., the waveguide with the scatterer absent. In view of Eq. (3.8), the following waveguide problems can be identified:

Case 1: Empty waveguide (with a point source)

Considering a harmonic omni-directional point source at $r = 0$ and $z = z_s$ in the waveguide, the forced Helmholtz equation may be written, using Eq. (3.6), as (Jensen et al., 2011),

$$\rho(r,z)\frac{1}{r}\frac{\partial}{\partial r}\left(\frac{1}{\rho}r\frac{\partial p_I}{\partial r}\right)+\rho(r,z)\frac{\partial}{\partial z}\left(\frac{1}{\rho}\frac{\partial p_I}{\partial z}\right)+\left(\frac{\omega^2}{c^2(r,z)}\right)p_I = S_0\frac{\delta(r)\delta(z-z_s)}{2\pi r} \tag{3.9}$$

where δ denotes the Dirac delta function. Note that Eq. (3.9) governs cylindrically symmetric wave propagation in a range and depth dependent waveguide containing a point source on the axis of the cylinder.

Case 2: Rigid scattering problem

It is important to note that while the solution to Eq. (3.9) represents an axisymmetric pressure field, the pressure distribution on the surface S_{IF} of an imaginary scatterer located at (r_B, z_B) will be nonaxisymmetric with respect to the vertical axis of revolution of the scatterer. Thus, the rigid scattering problem, despite the axisymmetry of the scatterer, is indeed a nonaxisymmetric problem. Fortunately, choosing a suitable coordinate system, the incident pressure on the surface S_{IF} may be expressed as a Fourier series as in Eq. (3.5). For this purpose, consider a cylindrically symmetric waveguide in a new coordinate system, $(\bar{r}, z)$ with the axisymmetric scatterer located at $\bar{r} = 0$ and at depth z_B (see Fig. 3.1). It is evident that the radial coordinate in Case 1 above is related to the radial coordinate here as $\bar{r} = r - r_B$ .Then, the incident pressure field may be written following Eq. (3.5) as,

$$p_I(\bar{r}, z, \theta) = \sum_{m=-\infty}^{m=\infty} p_{\mathrm{I,m}}(\bar{r}, z)\exp(im\theta) \tag{3.10}$$

And the pressure due scattered waves p_{Rs0} in Eq. (3.8b) may be written as,

$$p_{Rs0}(\bar{r}, z, \theta) = \sum_{m=-\infty}^{m=\infty} p_{Rs0,m}(\bar{r}, z)\exp(im\theta) \tag{3.11}$$

Then, the boundary condition on the surface of the scatterer is given by

$$\frac{\partial p_{Rs0,m}}{\partial n} = -\frac{\partial p_{\mathrm{I,m}}}{\partial n} \text{ on } S_{IF} \tag{3.12}$$

where n is normal to the surface of the scatterer. The governing equation for this waveguide problem follows from Eq. (3.6) as,

$$\rho(r,z)\frac{1}{r}\frac{\partial}{\partial r}\left(\frac{1}{\rho}r\frac{\partial p_{Rs0,m}}{\partial r}\right)+\rho(r,z)\frac{\partial}{\partial z}\left(\frac{1}{\rho}\frac{\partial p_{Rs0,m}}{\partial z}\right)+\left(\frac{\omega^2}{c^2(r,z)}-\frac{m^2}{r^2}\right)p_{Rs0,m}=0 \tag{3.13}$$

The forcing for this problem comes from the interface condition in Eq. (3.12).

Case 3: Radiation problem

As discussed in Sec. 2.3, when the body is elastic, it vibrates due to the acoustic pressure loading on it; this effect can be represented as a *radiation problem*, in which acoustic waves are generated because of structural motion at the body-fluid interface. This waveguide also has $\bar{r}$ as the range coordinate, as in Case 2 above. The radiated pressure may also be written (see Eq. (3.11)) as,

$$p_{Rad}(\bar{r},z,\theta)=\sum_{m=-\infty}^{m=\infty}p_{Rad,m}(\bar{r},z)\exp(im\theta) \tag{3.14}$$

Then, the boundary condition on the surface of the radiator is given by

$$\frac{\partial p_{rad,m}}{\partial n}=p_{mv} \tag{3.15}$$

At this stage it is important to recall that the elastic scattering problem being a coupled one involving fluid dynamic and the structural dynamic equations, the amplitude of normal velocity field can assumed to be unity, but its distribution on the surface of the radiator should be specified using certain assumed modes. Recalling Sec. 2.5, this problem can be tackled following one of the subsequent approaches:

1. If the in-vacuo structural dynamic problem has an exact solution, the mode shapes are known analytically. Several problems involving the vibration of cylindrical and spherical shells are discussed in Junger and Feit (1972).

2. An assumed mode approximation may be used when the structural dynamic equations are not amenable to exact solution. This approach has been outlined in Chapter 2.

3. For complex structural forms, the dry mode shapes of vibration may be generated using a finite element model. Then, in order to follow the simplified procedure discussed in Chapter 2 for solving the radiation problem, an assumed approach may be adopted. The assumed modes may be fitted to the mode shapes of vibration derived from the FE model employing a least squares method.

The governing equation for this waveguide problem follows from Eq. (3.6) as,

$$\rho(r,z)\frac{1}{r}\frac{\partial}{\partial r}\left(\frac{1}{\rho}r\frac{\partial p_{Rad,m}}{\partial r}\right)+\rho(r,z)\frac{\partial}{\partial z}\left(\frac{1}{\rho}\frac{\partial p_{Rad,m}}{\partial z}\right)+\left(\frac{\omega^2}{c^2(r,z)}-\frac{m^2}{r^2}\right)p_{Rad,m}=0 \tag{3.16}$$

The forcing for this problem evidently comes from the interface condition in Eq. (3.15).

3.3 Radiation Condition at the Truncation Boundary

Wave propagation problems require suitable radiation boundary condition to ensure that the waves are truly outgoing. In linear problems, the well-known Sommerfield radiation condition, which is a limiting condition, is commonly used. Domain discretization methods such as the finite difference and FE methods applied to wave propagation problems necessarily require appropriate truncation of the problem domain. In order to approximate the radiation B.C on such truncation boundaries, several absorbing or nonreflecting boundary condition have been developed. In the present study, following Fix and Marin (1978) and Vendhan et. al (2010), the boundary damper operators due to Bayliss, Gunzberger and Turkel (BGT) (1982) are adopted for use in the FE model.

The BGT damper equation for a cylindrically symmetric wave may be written in a form similar to Eq. (3.7c). The first order cylindrical damper equation may be written on the truncation boundary S_R as

$$\frac{\partial p_m}{\partial r} + a p_m = 0 \text{ on } S_R \tag{3.17}$$

where for exterior harmonic acoustic problems, $a = -ik$, the medium wavenumber. On the other hand, in waveguide acoustics, a finite number (say n) of radial modes, with associated wave numbers, travel outward, and hence Eq. (3.17) needs to be satisfied for each of them (Fix and Marin, 1978 and Vendhan et al., 2010). Thus, for cylindrical waveguides, Eq. (3.17) may be written as

$$\frac{\partial p_{mj}}{\partial r} + \alpha_j p_{mj} = 0 \text{ on } S_R \tag{3.18a}$$

where

$$\alpha_j = \left(\frac{1}{2r} - ik_{rj} \right), j = 1, 2, 3... \tag{3.18b}$$

In Eq. (3.18b), k_{rj}, $j = 1, 2, 3...$, n denote the radial/horizontal wavenumbers. For depth dependent waveguides, the horizontal wavenumbers k_{rj} and the associated depth modes $f_j(z)$ can in general be obtained numerically. It is well known the normal mode solution for such a waveguide may be written, at a given range, as

$$p_m(z) = \sum_{j=1}^{n} a_j f_j(z) \tag{3.19}$$

where the modal coefficients a_j may be obtained using the orthogonality of the depth modes/eigenmodes. In view of Eq. (3.19), the absorbing boundary conditions in Eq. (3.18a) may be written as

$$\frac{\partial p_m}{\partial r} + \sum_{j=1}^{n} a_j \alpha_j f_j(z) = 0 \tag{3.20}$$

3.4 Variational Formulation

In order to facilitate finite element modeling, a variational formulation equivalent to Eq. (3.6) together with appropriate boundary conditions is chosen here. Consider the functional given by

$$I(r,z)=\frac{1}{2}\int_{\Omega}\frac{1}{\rho(r,z)}\left[\left(\frac{\partial\overline{p}}{\partial r}\right)^2+\left(\frac{\partial\overline{p}}{\partial z}\right)^2\right]r\,dr\,dz-\frac{1}{2}\int_{\Omega}\frac{1}{\rho(r,z)}\left(\frac{\omega^2}{c^2(r,z)}-\frac{m^2}{r^2}\right)\overline{p}^2\,r\,dr\,dz$$
$$-\int_{S_D+S_N}\frac{1}{\rho(r,z)}\frac{\partial\overline{p}}{\partial n}\overline{p}+\frac{1}{2}\sum_{j=1}^{M}\frac{1}{\rho(r,z)}\int_{S_R}\left(\alpha_j\overline{p}^2\right)r\,dz \qquad (3.21)$$

For Case 1 defined Sec. 3.2,

$$m=0 \text{ and } \overline{p}=p_{I,m} \qquad (3.22a)$$

where the point source at $r=0$ provides the excitation.

For Case 2 defined in Sec. 3.2,

$$\overline{p}=p_{Rs0,m} \qquad (3.22b)$$

the *m*-th harmonic component of scattered pressure. The B.C. on the scattering body is given by Eq. (3.12).

For Case 3 defined in Sec. 3.2,

$$\overline{p}=p_{Rad,m} \qquad (3.22c)$$

the *m*-th radiated acoustic pressure. The body B.C. given by Eq. (3.15).

It can be shown that stationarity condition

$$\overline{\delta} I=0 \qquad (3.23)$$

For the functional in Eq. (3.21) leads to the governing equation and the associated boundary conditions discussed above.

3.5 Steps in Elastic Scattering Analysis

In order to provide a better understanding of the computational model discussed above, a flow chart of the various steps is given in Figs. 3.2a and 3.2b.

STEP 1

Waveguide coordinates: (r, z)

Solve empty waveguide with point source at $r = 0$ to find p_I

(This is an axisymmetric WG analysis)

Find $\frac{\partial p_I}{\partial n}$ on the imaginary surface of the scatterer

(This will be nonaxisymmetric w.r.t. body axis))

STEP 2

Waveguide coordinates: $(\bar{r}, z)$

Body centered at $\bar{r} = 0$

Perform nonaxisymmetric WG analysis to find rigid scattered pressure p_{RS}.

Body boundary condition (Eq. (3.12))

$$\frac{\partial p_{RS}(\bar{r}, z)}{\partial n} = -\frac{\partial p_I(\bar{r}, z)}{\partial n}$$

Find generalized load vector due to scattered pressure (see Eq. 2.16)

Fig. 3.2a Steps in Rigid Scattering Analysis

STEP 3 (repeated for *m* = 1,2,..)

Waveguide coordinates $(\bar{r}, z)$

Body centered at $\bar{r} = 0$

Perform nonaxisymmetric WG analysis to find radiated pressure p_{Radj} due to assumed mode j with unit amplitude of pressure gradient on the scatterer surface.

Body boundary condition : $\frac{\partial p_{Radj}(\bar{r}, z)}{\partial n} = f_j(\bar{r}, z)$

Find acoustic radiation load matrix F_{jk} (see Eq. 2.21)

Derive added mass and radiation damping matrices from F_{jk} (see Eq. 2.22)

Fig. 3.2b Steps for Setting up Added Mass and Radiation Damping Matrices

Chapter 4
Finite Element Analysis of Depth and Range Dependent Waveguides

4.1 Finite Element Model

The variational problem in Eq. (3.21) may be solved by extending the finite element model in Vendhan et al (2010) to nonzero circumferential harmonics, i.e., $m \geq 0$. An 8-node isoperimetric quadrilateral element has been adopted in the FE formulation. The acoustic pressure $\bar{p}$ in a finite element may be written as

$$\bar{p}(r,z) = \sum_{j=1}^{\bar{m}} \tilde{p}_{ej} N_j(\xi,\varsigma) = [N]\{\tilde{p}_e\} \tag{4.1}$$

where N_j denotes a polynomial shape function in terms of the parametric coordinates (ξ,ς) in the (r,z) plane and $\tilde{p}_{ej}$ the acoustic pressure at the *j*-th node of an *m*-node finite element. For details of isoparametric quadrilateral element formulation see Cook et al. (2004). Upon using Eq. (4.1) in Eq. (3.21), the following discrete approximation for the functional is obtained:

$$I(\tilde{p}_e) \approx \frac{1}{2}\{\tilde{p}_e\}^T \left([K_e]-[M_e]\right)\{\tilde{p}_e\} + \frac{1}{2}\sum_{m=1}^{N}\{\tilde{p}_{em}\}^T \left[\bar{R}_{em}\right]\{\tilde{p}_{em}\} - \{\tilde{p}_e\}^T\{f_e\} \tag{4.2}$$

The stationarity condition (see Eq. (3.23)) on the potential $I(\tilde{p}_e)$ in Eq. (4.2) should be subjected to the constraint so as to impose the boundary damper condition in Eq. (3.18). The damper equation in (3.18) may be written (at $r = r_B$, the radiation boundary S_R) as

$$[C]\left\langle \bar{p}(r_B,z),\ a_1\ a_2,\ ...a_n \right\rangle^T = 0 \tag{4.3a}$$

where,

$$[C] = [1, -f_1(z), -f_2(z), ... - f_n(z)] \tag{4.3b}$$

In Eq. 4.3a, a_j are the unknown modal coefficients associated with the depth modes $f_j(z)$.

Adopting the penalty function approach discussed in Vendhan et al. (2010), this may be achieved by constructing a modified potential as

$$I' = I + \frac{1}{2}\{\tilde{p}'_e\}^T [C_e]^T [\beta_p][C_e]\{\tilde{p}'_e\} \tag{4.4a}$$

i.e.

$$I'(\tilde{p}'_e) \approx \frac{1}{2}\{\tilde{p}'_e\}^T \left([K'_e]-[M'_e]+[R'_e]+[C_e]^T[\beta_p][C_e]\right)\{\tilde{p}'_e\} - \{\tilde{p}'_e\}^T\{f_e\} \tag{4.4b}$$

where the expanded nodal dof array is given by

$$\{\tilde{p}'_e\} = \begin{Bmatrix} \{\tilde{p}_e\} \\ \{a\} \end{Bmatrix} \tag{4.5}$$

The various matrices in Eq. (4.4b) are given by

$$\left[K_e'\right]=\begin{bmatrix}\left[K_e\right] & 0\\ 0 & 0\end{bmatrix};\left[M_e'\right]=\begin{bmatrix}\left[M_e\right] & 0\\ 0 & 0\end{bmatrix};\left[R_e'\right]=\begin{bmatrix}0 & 0\\ 0 & \left[R_e\right]\end{bmatrix};\left\{f_e'\right\}=\begin{Bmatrix}\left\{f_e\right\}\\ 0\end{Bmatrix} \tag{4.6a}$$

$$\left[K_e\right]=\int_{\Omega_e}\frac{1}{\rho}\nabla\left[N\right]^T\nabla\left[N\right]d\Omega \tag{4.6b}$$

$$\left[M_e\right]=\int_{\Omega_e}\frac{k^2}{\rho}\left[N\right]^T\left[N\right]d\Omega \tag{4.6c}$$

$$\left[R_e\right]=diag\left[R_{e1},R_{e2},...R_{eM}\right] \tag{4.6d}$$

$$R_{em}=\left\{f_{zm}\right\}^T\left[\bar{R}_{em}\right]\left\{f_{zm}\right\};\left[\bar{R}_{em}\right]=\alpha_m\int_{S_{\mathrm{Re}}}\frac{1}{\rho}\left[N\right]^T\left[N\right]dS \tag{4.6e}$$

$$\left\{f_{zm}\right\}=\left\langle f_{zm}(z_1),\ f_{zm}(z_2),.....f_{zm}(z_n)\right\rangle^T \tag{4.6f}$$

$$\left\{f_e\right\}=\int_{S_{Ne}}\frac{1}{\rho}p_v\left[N\right]^T dS \tag{4.6g}$$

where $\left[K_e\right]$, $\left[M_e\right]$ and $\left[R_e\right]$ are formally known as the element stiffness, mass and radiation damping matrices, and $\left\{f_e\right\}$ denotes the element load vector. The stationarity condition in Eq. (3.23) is replaced by the following condition

$$\frac{\partial I'}{\partial\left\{p_e'\right\}}=0 \tag{4.7}$$

which leads to the matrix equation

$$\left(\left[K_e'\right]-\left[M_e'\right]+\left[R_e'\right]+\left[C_e\right]^T\left[\beta_p\right]\left[C_e\right]\right)\left\{\tilde{p}_e'\right\}=\left\{f_e'\right\} \tag{4.8}$$

The finite element assemblage operation using the element equations in (4.6) leads to the global FE equation given by

$$\left(\left[K'\right]-\left[M'\right]+\left[R'\right]+\left[C'\right]\right)\left\{\tilde{p}'\right\}=\left\{f'\right\} \tag{4.9}$$

where

$$\left[K'\right]=\sum_e\left[K_e'\right];\left[M'\right]=\sum_e\left[M_e'\right];\left[R'\right]=\sum_e\left[R_e'\right] \tag{4.10a}$$

$$\left[C'\right]=\sum_e\left[C_e\right]^T\left[\beta_p\right]\left[C_e\right];\left\{f'\right\}=\sum_e\left\{f_e'\right\} \tag{4.10b}$$

with $\sum_e$ denoting the assemblage operation.

4.2 Solution of the FE Equations

The linear matrix equation in (4.9) resulting from the FE model for waveguide propagation may be written as

$$[A]\{p\} = \{f\} \tag{4.11}$$

The matrix [*A*] is symmetric and positive definite. A FORTRAN 90 code has been developed as a part of the present study, implementing the FE model for the modal Helmholtz equation for solving both rigid scattering and radiation problems. A block-storage banded Gauss solver has been employed to solve Eq. (4.11). For large FE models, iterative solvers based on the conjugate gradient method would be computationally more efficient. However, it should be remembered that the capability of the Gauss solver to handle multiple load vectors with a single factorization could be exploited for solving radiation problems involving many assumed modes. As indicated in Eq. (3.12), the normal derivative of the incident pressure field needs to be calculated from the FE solution. Since the FE model in Eq. (4.1) denotes a C_0 model, calculation of derivatives requires special procedures which are analogous to methods employed for stress calculation from FE solution to elasticity problems (Cook et al., 2004).

4.3 Depth Eigenproblem

The mathematical model that forms the basis for the FE model is based on the assumption that in the vicinity of the truncation boundary and beyond the waveguide has constant depth and the acoustic properties are only depth dependent. Thus the FE model requires depth eigensolution at the truncation boundary. For this purpose, Eq. (3.6) may first be reduced to the following form assuming depth dependent properties:

$$\rho(r)\frac{1}{r}\frac{\partial}{\partial r}\left(\frac{1}{\rho}r\frac{\partial p_m}{\partial r}\right)+\rho(r)\frac{\partial}{\partial z}\left(\frac{1}{\rho}\frac{\partial p_m}{\partial z}\right)+\left(\frac{\omega^2}{c^2(z)}-\frac{m^2}{r^2}\right)p_m = 0 \tag{4.12}$$

Assuming a variable separable solution in the form

$$p_m(r,z) = R(r)Z(z) \tag{4.13}$$

Eq. (4.12) may be written as

$$\frac{\rho\frac{1}{r}\frac{\partial}{\partial r}\left(\frac{1}{\rho}r\frac{\partial R}{\partial r}\right)-\frac{m^2}{r^2}R}{R}+\frac{\rho\frac{\partial}{\partial z}\left(\frac{1}{\rho}\frac{\partial Z}{\partial z}\right)+\frac{\omega^2}{c^2}Z}{Z} = 0 \tag{4.14}$$

Then, the depth eigenproblem for the axisymmetric waveguide with nonaxisymmetric acoustic field in the form given by Eq. (4.13), of course with only depth dependence, may be deduced from Eq. (4.14) as

$$\rho \frac{\partial}{\partial z}\left(\frac{1}{\rho}\frac{\partial Z}{\partial z}\right)+\left(\frac{\omega^2}{c^2}-k_r^2\right)Z=0 \tag{4.15}$$

where k_r denotes the radial wavenumber. Eq. (4.15) is evidently identical to the case of axisymmetric wave field. The depth modes $Z_j\,(\equiv f_j)$ and radial wavenumbers k_{rj} may readily be obtained using the KRAKEN code [Porter, 2001], which employs a finite difference model to discretize the depth equation in (4.15). However, in the present study, a Rayleigh-Ritz (RR) model has been developed to obtain the eigensolution, in which the depth modes appear in a compact form as a linear combination of the isovelocity mode shapes. Such a form for the mode shapes has been found to be more convenient to use in the proposed FE model. The details of the RR model for the depth eigenvalue problem and numerical validation are presented in Chapter 5.

Chapter 5

Rayleigh-Ritz Approximation to Depth Eigenvalue Problem of Shallow Water Acoustic Waveguides

5.1 Introduction

The sound speed in an ocean acoustic waveguide is in general both depth and range dependent. Depth dependence is considered very important because it is responsible for many interesting phenomena in waveguide propagation. The two well-known methods that have been developed to study acoustic waves in depth dependent waveguides are the fast-field technique and the normal mode expansion (Frisk, 1994; Jensen et al., 2011), the latter being the subject matter of the present paper. The normal mode approach consists of first solving the depth eigenvalue problem for a given sound speed profile to obtain the radial wavenumbers and the associated depth modes, which respectively are the eigenvalues and eigenfunctions. The depth eigenproblem could be solved exactly only for a few cases. So, several numerical methods have been developed to solve the depth problem (Jensen et al., 2011). The KRAKEN code (Porter, 2001) employs a finite difference model for the depth equation and the resulting algebraic eigenproblem has been solved using a combination of iterative techniques and Richardson extrapolation to obtain the radial wavenumbers and modal vectors to a great degree of precision (Porter and Reiss, 1984). Given the depth eigensolution, the acoustic field in the waveguide can be obtained using the well-known normal mode approach (Kinsler et al., 2000, Porter, 2001; Jensen, 2011). The KRAKEN code has been used extensively in the ocean acoustic community for both shallow and deep water waveguides. In the finite element model for depth and range dependent waveguides (Fix and Marin, 1978; Vendhan et al., 2010), the eigenvalue solution of the depth problem is required for imposition of the radiation condition at the truncation boundary. In the Couple method (Evans, 1984), the depth eigenvalue solution is required at every range independent strip, a series of which makeup a range dependent waveguide. For the foregoing applications, it would be convenient to have the depth modes in a compact form. The main thrust of the present paper is to explore this aspect with specific reference to shallow water waveguides.

The depth eigenvalue problem can be cast in a variational form by suitably defining a functional. Then, the classical Rayleigh-Ritz (RR) method, widely used to find approximate solutions of eigenvalue problems in structural mechanics, may be employed to find a variational approximation to the eigenvalue solution of the depth problem in ocean acoustic waveguides. The depth modes obtained would have a more compact form than those derived using finite difference or even finite element methods. There seems to be no study dealing with this approach. The present paper provides a RR model for the depth eigenvalue problem and demonstrates its accuracy for shallow water waveguides. The numerical features of the RR model are brought out by applying it to both single and two layer waveguides.

The depth equation for an acoustic waveguide overlying a fluid halfspace is presented in Sec. 5.2. A variational formulation for the depth problem is presented and a RR approximation to the depth eigensolution is discussed in Sec. 5.3. Sec. 5.4 provides a brief overview of the numerical aspects of the RR model, and its application to both single and two layer shallow water waveguides. Salient features of the RR model are discussed and results based on this model are compared with the exact solution and numerical results from KRAKEN. Sec. 5.5 reviews the RR model presented and its possible extensions.

5.2 Mathematical Model

Consider a cylindrically symmetric waveguide having depth dependent density ρ and sound speed c. A homogeneous acoustic fluid half-space is assumed to underlie the OAWG. The OAWG is assumed to be the inhomogeneous, and the pseudo Helmholtz equation governing the linear harmonic acoustic pressure field $p(r,z)$ in the waveguide. It is given in cylindrical coordinates (r,z) as (Frisk, 1994; Jensen et al., 2011)

$$\frac{1}{r}\frac{\partial}{\partial r}\left(r\frac{\partial p}{\partial r}\right)+\rho(z)\frac{\partial}{\partial z}\left(\frac{1}{\rho(z)}\frac{\partial p}{\partial z}\right)+\frac{\omega^2}{c^2(z)}p=-\frac{\bar{\delta}(r)\bar{\delta}(z-z_s)}{2\pi r} \tag{5.1}$$

where r denotes the range coordinate and z the depth coordinate as shown in Fig. 5.1, and the *r.h.s.* denotes a point source of unit amplitude located at $r = 0$ and $z = z_s$, with $\bar{\delta}$ denoting the Dirac delta function.

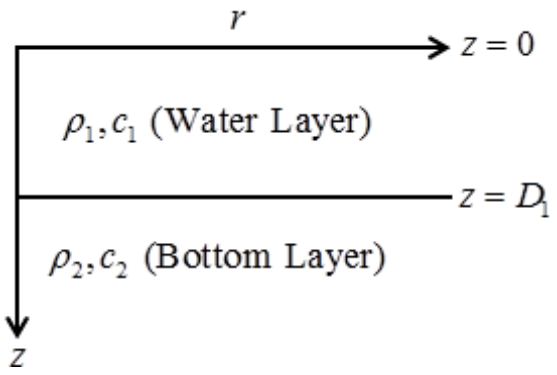

Figure 5.1 A two layer waveguide

Eq. (5.1) can also be applied to problems with attenuation by introducing a complex sound speed. In order to set up the normal mode solution of Eq. (5.1), a variable separable solution of the homogeneous form of Eq. (5.1) may be written as

$$p(r,z)=\bar{R}(r)Z(z) \tag{5.2}$$

Then, upon using Eq. (5.2) in the homogeneous form of Eq. (5.1), the following ordinary differential equations are obtained (see Sec. 4.3):

$$\frac{1}{r}\frac{d}{dr}\left(r\frac{d\bar{R}(r)}{dr}\right)+k_r^2\bar{R}(r)=0 \tag{5.3}$$

$$\rho(z)\frac{d}{dz}\left(\frac{1}{\rho(z)}\frac{dZ(z)}{dz}\right)+\left(\frac{\omega^2}{c^2(z)}-k_r^2\right)Z(z)=0 \tag{5.4}$$

where ω denotes the circular frequency and k_r^2 the separation constant, which turns out to be the square of the radial/horizontal wavenumber. Eq. (5.3) evidently pertains to the radial/horizontal modes $\bar{R}(r)$ and Eq. (5.4), which is of main concern in the present paper, pertains to the depth modes $Z(z)$. Choosing a pressure release boundary at the top ($z=0$) and a mixed/Robin boundary condition at the seabed ($z=D_1$), they may be written as (Jensen, 2011; Porter, 2001),

$$Z(0)=0 \tag{5.5}$$

$$Z(D_1)+\frac{g\left(k_r^2\right)}{\rho}\frac{dZ}{dz}=0 \tag{5.6a}$$

where

$$g\left((k_r^2\right)=\rho_b\,/\sqrt{\left(k_r^2-\frac{\omega^2}{c^2}\right)} \tag{5.6b}$$

with ρ_b denoting the density of the acoustic fluid in the isovelocity half-space underlying the water column. Eq. (5.6) facilitates replacing the half-space in the Pekeris waveguide (Pekeris, 1948) by means of an impedance type boundary condition. It is interesting to note that Eq. (5.4) together with the homogeneous boundary conditions in Eq. (5.5) and Eq. (5.6a) does not constitute a proper Sturm-Liouville problem because Eq. (5.6a) depends on the unknown eigenvalue k_r^2. In the KRAKEN code, a finite difference model is employed to solve Eq. (5.4) together with the boundary conditions in Eq. (5.5) and Eq. (5.6).

As an alternative to Eq. (5.6a), the depth equation for the fluid half-space is considered here. Noting Eq. (5.1), for the half-space,

$$\rho_b(z)\frac{d}{dz}\left(\frac{1}{\rho_b(z)}\frac{dZ_b(z)}{dz}\right)+\left(\frac{\omega^2}{c_b^2(z)}-k_r^2\right)Z_b(z)=0,\;\; D_1\le z\le\infty \tag{5.7}$$

where Z_b denotes the depth function in the fluid half-space having depth dependent density ρ_b and sound speed c_b.The interface conditions at the seabed are given by the kinematic and dynamic conditions,

$$Z(D_1) = Z_b(D_1) \tag{5.8a}$$

$$\frac{1}{\rho}\frac{dZ(D_1)}{dz} = \frac{1}{\rho_b}\frac{dZ_b(D_1)}{dz} \tag{5.8b}$$

In addition, the depth mode Z_b should remain bounded as $z \to \infty$. The objective here is to consider a variational formulation for Eq. (5.4) and Eq. (5.7) together with appropriate boundary conditions and obtain a RR approximation to the depth problem.

5.3 Variational Formulation and Rayleigh-Ritz Approximation

A variational formulation equivalent to the boundary value problem in Sec. 5.2 is sought now. The operator being symmetric, there exists a functional, the variation of which leads to Eq. (5.4) and appropriate boundary conditions, and similarly for the half-space. Consider the functional $\prod(Z)$ and $\prod_b(Z_b)$ defined respectively in the water column and the half-space as

$$\prod(Z) = \frac{1}{2}\int_0^{D_1}\left[\frac{1}{\rho(z)}\left(\frac{dZ}{dz}\right)^2 - \frac{\omega^2}{\rho(z)c^2(z)}Z^2 + \frac{1}{\rho(z)}k_r^2(z)Z^2\right]dz - \frac{1}{\rho(z)}Z_\upsilon Z\Big|_0^{D_1} \tag{5.9}$$

$$\begin{aligned}\prod_b = \frac{1}{2}\int_{D_1}^{D_2}\left[\frac{1}{\rho_b(z)}\left(\frac{dZ_b}{dz}\right)^2 - \frac{\omega^2}{\rho_b(z)c^2(z)}Z_b^2 + \frac{1}{\rho_b(z)}k_r^2 Z_b^2\right]dz \\ -\frac{1}{\rho_b(z)}Z_{b\upsilon}(D_1)Z_b(D_1) + \frac{1}{2}\beta\frac{Z_b^2(D_2)}{\rho_b},\ D_2 \to \infty\end{aligned} \tag{5.10}$$

At the interface $z = D_1$ between the water column and the half-space, the conditions noted in Sec. 5.2 must be imposed. In view of Eq. (5.8b), this can be achieved by setting in Eq. (5.9)

$$\frac{1}{\rho}Z_\nu(D_1) = \frac{1}{\rho_b}\frac{dZ(D_1)}{dz}; \tag{5.11}$$

and in Eq. (5.10),

$$\frac{1}{\rho_b}Z_{b\nu}(D_1) = \frac{1}{\rho}\frac{dZ(D_1)}{dz} \tag{5.12}$$

In addition, Eq. (5.8a) should be imposed. Then, it can easily be shown that the variational condition $\delta\prod = 0$ leads to Eq. (5.4) and the boundary conditions in Eq. (5.5) as well as the interface condition in Eq. (5.11), where δ denotes the first variation. Similarly, the variational condition $\delta\prod_b = 0$ leads to Eq. (5.7), and the interface conditions in Eq. (5.8a) and Eq. (5.12). In addition, at $z = D_2$ we obtain the condition

$$\frac{dZ_b(D_2)}{dz} + \beta Z_b(D_2) = 0 \tag{5.13a}$$

where, noting Eq. (5.6), for a homogeneous half-space,

$$\beta = \frac{\rho}{\rho_b} \frac{1}{g\left((k_r^2\right)} \tag{5.13b}$$

Note that for waveguides with a finite depth fluid layer under the water column, the last term in Eq. (5.10) is deleted and D_2 would be finite.

We now seek an assumed mode solution with *n* terms to the above variational problem in the form

$$Z(z) \approx \sum_{j=1}^{n_1} \overline{\phi}_j \psi_j(z), \qquad 0 \le z \le D_1 \tag{5.14a}$$

$$Z_b(z) \approx \sum_{j=1}^{n_2} \overline{\phi}_{bj} \psi_{bj}(z) \quad D_1 \le z \le \infty \tag{5.14b}$$

where ψ_j denotes a known coordinate function satisfying the kinematic boundary condition in the water column and $\overline{\phi}_j$ an unknown constant, and their counterparts with suffix *b* correspond to the half-space. Let the two sets of coordinate function above be such that they satisfy the interface conditions in Eq. (5.8) and the condition in Eq. (5.13). Such functions may readily be constructed by solving a two layer depth problem, (which is nothing but the Pekeris waveguide), with an appropriate choice of constant velocity and density in the water column and the half-space. This approach has been adopted here. Then, it follows that the continuity of pressure field at the interface $z = D_1$ implies that in Eq. (5.14)

$$\phi_j = \overline{\phi}_j, \quad n = n_1 = n_2 \tag{5.15}$$

Then, using Eq. (5.14) in the functional in Eq. (5.9) and Eq. (5.10) and combining them, an algebraic approximation for the functional is obtained as

$$\overline{\Pi} = \Pi + \Pi_b = \frac{1}{2}\left\{\overline{\phi}\right\}^T \left[K^I\right]\left\{\overline{\phi}\right\} - \frac{1}{2}\omega^2 \left\{\overline{\phi}\right\}^T \left[K^{II}\right]\left\{\overline{\phi}\right\} + \frac{1}{2}k_r^2 \left\{\overline{\phi}\right\}^T \left[K^{III}\right]\left\{\overline{\phi}\right\} \tag{5.16}$$

where

$$K_{ij}^{I} = \int_0^{D_1} \frac{1}{\rho(z)} \frac{d\psi_i}{dz} \frac{d\psi_j}{dz} dz + \int_{D_1}^{D_2} \frac{1}{\rho_b(z)} \frac{d\psi_{bi}}{dz} \frac{d\psi_{bj}}{dz} dz$$

$$K_{ij}^{II} = \int_0^{D_1} \frac{1}{\rho(z)c^2(z)} \psi_i \psi_j dz + \int_{D_1}^{D_2} \frac{1}{\rho_b(z)c_b^2(z)} \psi_{bi} \psi_{bj} dz \tag{5.17}$$

$$K_{ij}^{III} = \int_0^{D_1} \frac{1}{\rho(z)} \psi_i \psi_j dz + \int_{D_1}^{D_2} \frac{1}{\rho_b(z)} \psi_{bi} \psi_{bj} dz$$

It has been assumed in the above the contribution due to the last two terms in Eq. 5.10 is negligible as $D_2 \to \infty$.

The variational condition is now replaced by the condition

$$\frac{\partial \overline{\Pi}}{\partial \phi_j} = 0, \qquad j = 1, 2, ..., n \tag{5.18}$$

Eq. (5.18) yields a symmetric algebraic eigenproblem given by

$$\left(\omega^2 \left[K^{II}\right] - \left[K^{I}\right]\right)\left\{\overline{\phi}\right\} = k_r^2 \left[K^{III}\right]\left\{\overline{\phi}\right\} \tag{5.19}$$

The eigensolution of Eq. (5.19) may be denoted as

$$\left(k_{rj}^2, \left\{\phi^{(j)}\right\}\right), \; j = 1, 2, ..n \tag{5.20}$$

Having obtained the eigenvalues k_{rj}^2 and the eigenvectors $\left\{\overline{\phi}^{(j)}\right\}$, the eigenfunctions/depth modes may be written, using Eq. (5.14), as

$$Z_j(z) = \left\{\overline{\phi}^{(j)}\right\}^T \left\{\psi(z)\right\} \tag{5.21}$$

where

$$\left\{\psi(z)\right\}^T = < \psi_1(z), \psi_2(z), ..\psi_n(z) > \tag{5.22}$$

Eq. (5.21) provides a compact for the depth modes that are convenient to employ in FE models such as those in Fix and Marin (1978), Jensen et al. (2011), and Vendhan et al. (2010) for approximating the radiation condition at the truncation boundary. The depth modes obtained can of course be used to set up the normal mode solution to the forced Helmholtz equation in Eq. (5.1). Since the eigenvectors in Eq. (5.19) are $\left[K^{III}\right]$-orthogonal, it can easily be shown the eigenfunctions in Eq. (5.21) satisfy the following orthogonality condition:

$$\int_0^{D_1} \frac{1}{\rho(z)} Z_i Z_j dz + \int_{D_1}^{D_2} \frac{1}{\rho_b(z)} Z_i Z_j dz = 0 \tag{5.23}$$

In terms of finite element terminology, the RR model for each layer may be looked upon as a super element with C_1 continuity at the inter-element boundary and the operation leading to Eq. (5.16) is equivalent to element assemblage operation.

5.4 Numerical Analysis and Discussion

The Rayleigh-Ritz model in Sec. 5.3 has been implemented in MATLAB. The first task is to compute the symmetric matrices $\left[K^I\right]$, $\left[K^{II}\right]$ and $\left[K^{III}\right]$ in Eq. (5.17). The associated integrals have been evaluated using composite Gauss quadrature functions available in MATLAB. The next task is to find the eigensolution to Eq. (5.19). For problems with no attenuation, the real eigenvalues have been obtained employing the bisection method. For problems with attenuation, approximations to the complex roots have been obtained using a search procedure (Buckingham and Giddens, 2006) and the eigenvalues refined employing Newton-Raphson iteration. In all cases, the eigenvectors are obtained using inverse iteration.

The Rayleigh-Ritz model in Sec. 5.3 has been applied first to single layer isovelocity waveguide examples without attenuation for which exact solutions are available. The eigenvalues computed (not reproduced here for brevity) compared with the exact results better than 8 or 9 significant digits. This in essence provides validation of the numerical accuracy of the matrices $\left[K^I\right]$, $\left[K^{II}\right]$ and $\left[K^{III}\right]$ in Eq. (5.17), evaluated using numerical quadrature in MATLAB, especially for the half-space. Then, three different sound speed profiles (Sazontov; 2002; Schneider, 1977) shown in Fig. 5.2a-c have been chosen to evaluate the accuracy of the RR model. Attenuation in the fluid half-space has also been considered. Different sets of RR approximations have been obtained by varying the number of assumed modes n in Eq. (5.15). The results for $n = 2n_p$, where n_p denotes the number of propagating modes turned out to be of good accuracy and hence reproduced in Tables 1-6. All the examples studied have also been solved using a FORTRAN version of the KRAKEN code (Acoustics Tool Box), and the results compared with the present RR model. It is seen that most results compare up to 5 significant digits, and often better, which is deemed very good. Even the imaginary parts of the wavenumbers for the attenuating half-space problem compare fairly well. The modeshapes obtained by the two methods are indistinguishable to plotting accuracy, and hence not reproduced here.

The elements of the RR matrix, both in the finite layer and the semi-infinite layer, could be computed to a high degree of precision using MATLAB tools. The excellent performance of the RR model for the depth eigenproblem may be attributed to the following:

a) The modeshapes of an isovelocity waveguide have been chosen as trial functions, which satisfy appropriate interface conditions at the sea floor, and the boundary conditions at the free surface and finite bottom. This renders the RR matrix highly diagonally dominant, which also greatly aids in numerical evaluation of the eigensolution.
b) For ocean waveguides, the depth variation of the sound speed is normally only a small percentage of the nominal value.

5.3 Conclusion

A variational formulation for the depth problem of a shallow water Pekeris waveguide has been presented and eigensolution obtained using a Rayleigh-Ritz approximation, for low to medium frequency range. An interesting feature of the model is that the trial functions are derived from an isovelocity problem that has exact solution. It is important to note that such trial functions automatically satisfy even the dynamic interface condition at the seabed, thus contributing to the accuracy of the numerical model. The model has been implemented in MATLAB. The radial wavenumbers obtained compare very well with KRAKEN results. The proposed model is accurate and is deemed to provide a compact form for the depth modes as a linear combination of the isovelocity modes.

Admittedly, the computational effort in setting up the matrix in the proposed RR model using numerical quadrature is high compared to setting up the finite difference based matrix in the KRAKEN code. However, noting the diagonal dominance of the matrix obtained in the RR model, it would be worthwhile exploring the possibility of approximating it by a narrow banded matrix in order to reduce the volume of computation in setting up the matrix and possibly in obtaining the eigensolution.

The proposed RR model presented readily admits heterogeneous fluid halfspace, although only isovelocity cases have been studied. Extension of the Rayleigh-Ritz model to high frequency shallow water waveguides as well as medium and high frequency deep water waveguides would seem possible in principle. However, since such problems will have a few to several hundred modes, the performance of the RR model remains to be proved. Extension to shallow water geoacoustic waveguides would be worth investigating.

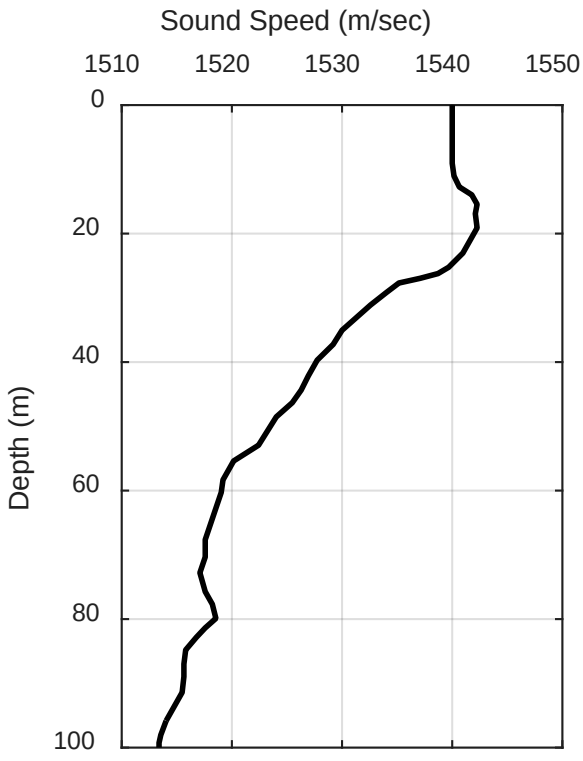

Figure 5.2(a) Sound speed profile-1

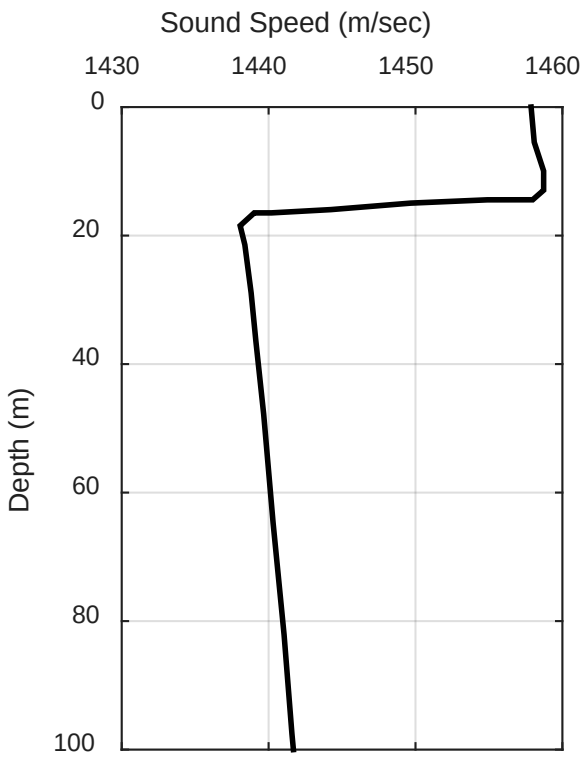

Figure 5.2(b) Sound speed profile-2 (Schneider, 1977)

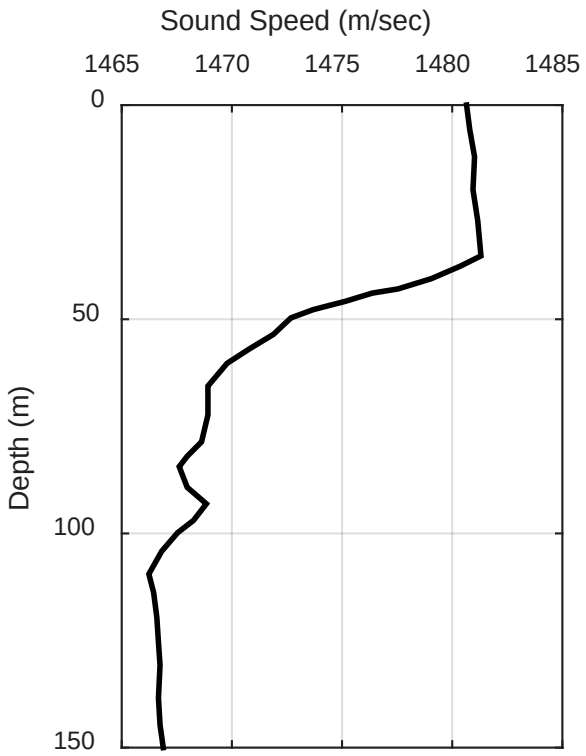

Figure 5.2c Sound speed profile-3 (Sazontov et al, 2002)

Chapter 6
Epilogue

6.1 Summary

The main thrust of this study has been to formulate a finite element model for elastic scattering by objects in a range and depth dependent cylindrical ocean acoustic waveguide. The 3-D wave equation for acoustic pressure has been chosen. Assuming time-harmonic motion, the acoustic field in the azimuthal direction has been expressed in a Fourier series, leading to a 2-D Helmholtz equation for each of the harmonics. The acoustic field due to linear elastic scattering by an axisymmetric body in the waveguide has been expressed as a sum of rigid-scattered and radiated acoustic fields. Harmonic acoustic radiation by an axisymmetric body has been discussed employing an assumed mode approach to structural displacements. The acoustic radiation (pressure) loading on the structure has been identified in terms of added mass and radiation damping matrices, which can be appended to the structural mass and damping matrices, thus completing the fluid-structure interaction formulation. The acoustic loading due to rigid-scattered field constitutes the forcing on the coupled system.

A finite element model has been formulated to solve the 2-D Helmholtz equation for each of the circumferential harmonics by truncating the fluid domain at a finite range. A Bayliss-type boundary operator has been adopted for each of the waveguide propagating modes, to serve as an approximate nonreflecting/absorbing condition on the truncation boundary. The proposed FE model applies to the empty waveguide with a point source, the waveguide embedded with a rigid scattering object and the waveguide with the scattering object considered as a radiator. The generalized FE model has been implemented in a FORTRAN90 code.
Depth eigensolution of the depth dependent waveguide is required to impose the nonreflecting boundary condition at the truncation boundary in the FE model. A Rayleigh-Ritz approximation has been developed for this purpose, using the depth eigenmodes of the isovelocity problem. The RR-model has been implemented using MATLAB coding.

6.2 Concluding Remarks

The FSI formulation for harmonic elastic scattering by axisymmetric objects in a waveguide conveniently decouples the acoustic/fluid dynamic formulation from the structural formulation, the former being the primary focus of this study. The FE model for the 2-D Helmholtz equation, despite being computationally intensive, readily accounts for complex axisymmetric geometries, multiple scattering and effect of free surface and seafloor.

It is interesting to note in the present study while an elaborate finite element model has been adopted for representing heterogeneous waveguide propagation, a classical approach has been indicated for modeling the vibration of axisymmetric scatterers, instead of a finite element model.

Despite its limitations, it is deemed that the structural formulation suggested provides a compact model, which in turn simplifies the finite element model for the waveguide radiation problem.

The Rayleigh-Ritz approximation developed for the depth eigenproblem yields eigenmodes as a linear combination of isovelocity modes. Such a form is more compact than the eigenmodes derived from finite difference or finite element models for the depth problem, and hence convenient to use with the FE model for the waveguide.

6.3 Further Research

The FORTRAN code developed in this study is fairly large in size and extensive testing has been done to validate different components of the numerical model. FE meshing and data generation code has been developed to exploit a commercially available standard FE preprocessor. As of now, coding for the radiation problem is complete and validation examples remain to be solved. The scattering problem involves extracting nonaxisymmetric scattered pressure on the surface of an axisymmetric body. Coding for this task is in progress. The research work reported here forms part of the doctoral work of the second author of this report. So, all the remaining tasks will be brought to a logical conclusion and included in the doctoral thesis.

Table 5.1 Propagating mode wavenumbers for 100 m deep single layer waveguide with pressure release top and rigid bottom, for sound speed profile-1 in Fig. 5.2a

Frequency 50 Hz			Frequency 100 Hz				Frequency 500 Hz				Frequency 1000 Hz		
j	Kraken	RR Model ($n = 2n_p$)	j	Kraken	RR Model ($n = 2n_p$)	j	Kraken	RR Model ($n = 2n_p$)	j	Kraken	RR Model ($n = 2n_p$)
1	0.20626 214	0.20626 201	1	0.41370 960	0.41370 970	1	2.07327 564	2.07327 560	1	4.14861 035	4.14861 026
2	0.20034 991	0.20034 985	2	0.40927 711	0.40927 704	2	2.06845 466	2.06845 461	2	4.14127 043	4.14127 031
3	0.19017 967	0.19017 943	3	0.40377 782	0.40377 775	3	2.06486 547	2.06486 537	3	4.13829 130	4.13829 125
4	0.17395 532	0.17395 521	6	0.37362 274	0.37362 269	29	1.85314 779	1.85314 761	64	3.60056 038	3.60056 011
5	0.14963 467	0.14963 417	7	0.35742 699	0.35742 694	30	1.83761 895	1.83761 876	65	3.58298 492	3.58298 469
6	0.11185 534	0.11185 467	8	0.33754 919	0.33754 916	31	1.82146 158	1.82146 144	66	3.56505 546	3.56505 524
7	0.02586 682	0.02586 071	11	0.24621 631	0.24621 595	64	0.50679 833	0.50679 799	129	0.80570 636	0.80570 489
			12	0.19734 847	0.19734 731	65	0.36129 618	0.36129 551	130	0.62813 151	0.62812 972
			13	0.12350 950	0.12350 583	66	0.04717 033	0.04716 571	131	0.37142 513	0.37142 194

Table 5.2 Propagating mode wavenumbers for 100 m deep single layer waveguide with pressure release top and rigid bottom, for sound speed profile-2 in Fig. 5.2b [10]

Frequency 50 Hz			Frequency 100 Hz				Frequency 500 Hz				Frequency 1000 Hz		
j	Kraken	RR Model ($n = 2n_p$)	j	Kraken	RR Model ($n = 2n_p$)	j	Kraken	RR Model ($n = 2n_p$)	j	Kraken	RR Model ($n = 2n_p$)
1	0.21750 372	0.21750 357	1	0.43587 227	0.43587 231	1	2.18221 704	2.18221 738	1	4.36602 483	4.36602 623
2	0.21290 853	0.21290 720	2	0.43359 244	0.43359 229	2	2.18053 321	2.18053 347	2	4.36375 413	4.36375 598
3	0.20324 210	0.20323 918	3	0.42871 517	0.42871 464	3	2.17934 145	2.17934 179	3	4.36201 332	4.36201 389
4	0.18792 005	0.18791 626	6	0.39951 802	0.39951 882	34	1.90610 439	1.90610 477	69	3.78584 771	3.78584 678
5	0.16548 007	0.16547 682	7	0.38456 842	0.38456 818	35	1.88843 941	1.88843 974	70	3.76780 058	3.76779 971
6	0.13237 311	0.13237 254	8	0.36632 398	0.36632 402	36	1.87008 454	1.87008 450	71	3.74945 258	3.74945 203
7	0.07556 731	0.07556 539	12	0.24303 274	0.24302 958	67	0.61368 851	0.61368 978	137	0.75886 488	0.75885 584
			13	0.18816 133	0.18815 815	68	0.49430 767	0.49430 752	138	0.55264 353	0.55263 741
			14	0.09895 384	0.09894 815	69	0.33193 990	0.33194 354	139	0.18167 275	0.18165 878

Table 5.3 Propagating mode wavenumbers for 150 m deep single layer waveguide with pressure release top and rigid bottom, for sound speed profile-3 [11]

Frequency 50 Hz			Frequency 100 Hz				Frequency 500 Hz			Frequency 1000 Hz		
j	Kraken	RR Model ($n = 2n_p$)	j	Kraken	RR Model ($n = 2n_p$)	j	Kraken	RR Model ($n = 2n_p$)	j	Kraken	RR Model ($n = 2n_p$)
1	0.21379 035	0.21379 031	1	0.42807 733	0.42807 730	1	2.14182 484	2.14182 465	1	4.28393 384	4.28393 346
2	0.21118 770	0.21118 766	2	0.42618 778	0.42618 772	2	2.14065 208	2.14065 178	2	4.28324 895	4.28324 844
3	0.20679 341	0.20679 334	3	0.42346 331	0.42346 321	3	2.13887 874	2.13887 849	3	4.28158 839	4.28158 770
4	0.20045 527	0.20045 521	8	0.39690 255	0.39690 250	49	1.87715 622	1.87715 607	100	3.72551 546	3.72551 528
5	0.19153 272	0.19153 267	9	0.38798 638	0.38798 633	50	1.86567 414	1.86567 401	101	3.71372 757	3.71372 738
6	0.17966 348	0.17966 341	10	0.37766 117	0.37766 108	51	1.85388 898	1.85388 886	102	3.70177 828	3.70177 810
7	0.16438 144	0.16438 129	11	0.36586 465	0.36586 456	52	1.84178 203	1.84178 192	103	3.68967 655	3.68967 636
8	0.14451 594	0.14451 157	18	0.21885 397	0.21885 275	100	0.46157 064	0.46157 029	202	0.64265 825	0.64265 713
9	0.11775 220	0.11775 171	19	0.17917 147	0.17916 949	101	0.35400 344	0.35400 296	203	0.48558 547	0.48558 401
10	0.07725 818	0.07725 680	20	0.12424 114	0.12423 713	102	0.19161 962	0.19161 871	204	0.24022 424	0.24022 120

Table 5.4 Propagating mode wavenumbers for two layer waveguide - top layer 100 m deep with sound speed profile-1; isovelocity bottom layer 50 m deep(ρ = 1024 kg/ m^3; $\rho_2 = 2000$ 0 kg/ m^3; $c_2 = 2000$ *m/s*)

Frequency 50 Hz			Frequency 100 Hz				Frequency 500 Hz			Frequency 1000 Hz		
j	Kraken	RR Model ($n = 2n_p$)	j	Kraken	RR Model ($n = 2n_p$)	j	Kraken	RR Model ($n = 2n_p$)	j	Kraken	RR Model ($n = 2n_p$)
1	0.20456 112	0.20456 103	1	0.41203 261	0.41203 272	1	2.07030 231	2.07030 222	1	4.14439 339	4.14439 290
2	0.19822 067	0.19822 067	2	0.40748 072	0.40748 071	2	2.06729 366	2.06729 348	2	4.13928 774	4.13928 750
3	0.18785 719	0.18785 687	3	0.40192 320	0.40192 319	3	2.06292 091	2.06292 079	3	4.13716 472	4.13716 405
4	0.17204 366	0.17204 356	7	0.35523 736	0.35523 732	45	1.56626 702	1.56627 064	90	3.12889 039	3.12889 046
5	0.15456 298	0.15456 313	8	0.33584 249	0.33584 244	46	1.56266 492	1.56266 466	91	3.12285 967	3.12285 252
6	0.14850 700	0.14850 645	9	0.31364 127	0.31364 508	47	1.55526 091	1.55526 088	92	3.11923 353	3.11924 959
7	0.12763 872	0.12763 890	16	0.19557 802	0.19557 645	89	0.38141 305	0.38141 320	179	0.62752 845	0.62753 139
8	0.10837 090	0.10836 998	17	0.14851 788	0.14851 899	90	0.29293 460	0.29293 311	180	0.47294 187	0.47293 210
9	0.05543 307	0.05543 244	18	0.10714 761	0.10713 932	91	0.04212 166	0.04212 181	181	0.32370 017	0.32370 695

Table 5.5 Wavenumbers for Pekeris waveguide example at 100 Hz [9]

(ρ = 1000 kg/ m^3 ; $c = 1500$ *m/s* ; $\rho_b = \rho_2 = 1250$ kg/ m^3 ; $c_2 = 1600$ *m/s*;Attenuation in half space = 0.3125 *db/km-Hz*)

j	Kraken	Ref. 9	RR Model(n = $2n_p$)
1	0.41585 560 + i 0.54834E−06	0.41585 35 + i0.0000547	0.41585 345 + i0.54674E−06
2	0.40668 711 + i 0.24050E−05	0.40668 12 + i0.0002392	0.40668 125 + i 0.23923E−05
3	0.39183 488 + i0.13149E−04	0.39184 12 + i0.0013215	0.39184 127 + i 0.13216E−04

Table 5.6 Propagating mode wave numbers for 100 m deep PEKERIS waveguide- sound speed profile-1 in water column (ρ = 1024 kg/m^3; $\rho_b = \rho_2 = 2000$ 0 kg/m^3; $c_2 = 2000$ *m/s*; Attenuation =0.3125 *db/km-Hz*) [9]

Frequency 50 Hz			Frequency 100 Hz				Frequency 500 Hz			Frequency 1000 Hz	
j	Kraken	RR Model ($n = 2n_p$)	*j*	Kraken	RR Model ($n = 2n_p$)	*j*	Kraken	RR Model ($n = 2n_p$)	*j*	Kraken	RR Model ($n = 2n_p$)
1	0.20456 091 + i0.10143E−06	0.20456 096 + i0.10111E−06	1	0.41203 246 + i0.63370E−07	0.41203 255 + i0.63402E−07	1	2.07030 219 + i 0.49511E−07	2.07030 211 + i 0.4545E−07	1	4.14439 324 + i 0.61407E−07	4.14439 277 + i 0.61452E−07
2	0.19822 000 + i0.25266E−06	0.19822 053 + i0.2536E−06	2	0.40748 043 + i0.12214E−06	0.40748 040 + i0.12227E−06	2	2.06729 356 + i0.40969E−07	2.06729 339 + i 0.40993E−07	2	4.13928 765 + i 0.35846E−07	4.13928 742 + i 0.35863E−07
3	0.18785 560 + i0.48573E−06	0.18785 605 + i0.4901E−06	3	0.40192 273 + i0.18618E−06	0.40192 272 + i0.18642E−06	3	2.06292 074 + i 0.67331E−07	2.06292 064 + i 0.67385E−07	3	4.13716 457 + i 0.56470E−07	4.13716 395 + i 0.56524E−07
4	0.17203 622 + i0.96521E−06	0.17204 994 + i0.9934E−06	4	0.39435 248 + i0.27286E−06	0.39435 260 + i0.27324E−06	20	1.96218 955 + i 0.31449E−06	1.96218 975 + i 0.31528E−06	41	3.91178 541 + i 0.33135E−07	3.91178 556 + i 0.33219E−06
			5	0.38427 786 + i0.40048E−06	0.38427 807 + i0.40110E−06	21	1.95219 366 + i 0.33974E−06	1.95219 396 + i 0.34062E−06	42	3.90148 034 + i 0.34428E−06	3.90148 040 + i 0.34519E−06
			6	0.37125 268 + i0.56060E−06	0.37125 300 + i0.56234E−06	22	1.94159 584 + i 0.36500E−06	1.94159 617 + i 0.36587E−06	43	3.89085 762 + i 0.35895E−06	3.89085 781 + i 0.35989E−06
			7	0.35523 437 + i0.79275E−06	0.35523 489 + i0.79506E−06	40	1.64060 761 + i 0.17135E−05	1.64061 287 + i 0.17410E−05	83	3.19707 658 + i 0.28194E−06	3.19709 962 + i 0.28947E−05
			8	0.33583 530 + i0.12559E−05	0.33583 538 + i0.12388E−05	41	1.61662 367 + i 0.21630E−05	1.61663 562 + i 0.21800E−05	84	3.17155 536 + i0.37810E−05	3.17159 690 + i 0.38429E−05
						42	1.59175 377 + i 0.32057E−05	1.59177 107 + i 0.32433E−05	85	3.14553 001 + i 0.77887E−05	3.14554 474 + i 0.76853E−05

Appendix

The Rayleigh-Ritz model presented for the depth eigenproblems, discussed in Sec. 5.3, employs the analytical depth modes for an isovelocity waveguide as the trial functions. The details of the various isovelocity waveguide examples used are presented here.

For a single layer waveguide shown in Fig. A.1, the trial functions are given by [1, 2, 5]

$$\psi_j = \sin(k_{zj} z), \text{ where } k_{zj} = \frac{(j-0.5)\pi}{D}, \; j = 1, 2, \ldots$$

For a *two layer waveguide* shown in Fig. A.2, the trial functions are given by [1]

$$\begin{aligned} \psi_i(z) &= a \sin k_{z1i} z && 0 \le z \le D_1 \\ &= a \frac{\sin k_{z1i} D_1}{\cos k_{z2i}(D_2 - D_1)} \cos k_{z2i}(D_2 - z) && D_1 \le z \le D_2 \end{aligned}$$

where $k_{z1i}^2 = \omega^2 / c_1^2 - k_r^2, k_{z2i}^2 = \omega^2 / c_2^2 - k_r^2$ and k_r is the solution of the transcendental equation

$$\frac{k_{zi1}\rho_2}{k_{zi2}\rho_1} = \tan k_{zi1} h_1 \tan k_{zi2} h_2$$

For a *Pekeris waveguide* (for which $D_2 \to \infty$ in Fig. A.2 the trial functions are given by [1, 2]

$$\begin{aligned} \psi_i(z) &= a \sin k_{z1i} z && 0 \le z \le D_1 \\ &= a \sin k_{z1i} h \, e^{-ik_{z2i}(h-z)} && D_1 \le z \le \infty \end{aligned}$$

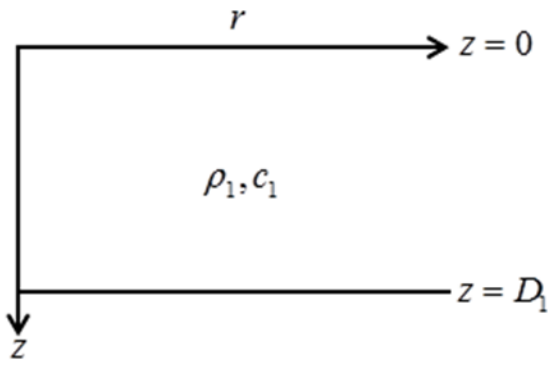

Figure A.1 Single layer waveguide

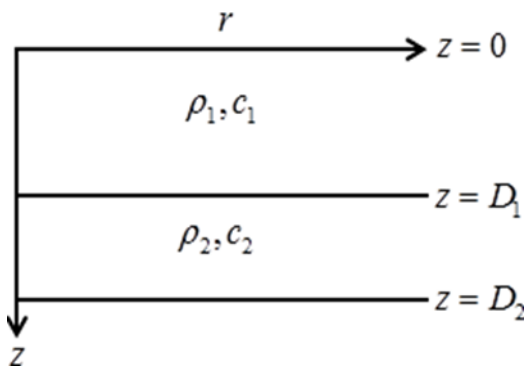

Figure A.2 Two layer waveguide

Acknowledgement: Partial financial support for the research work reported here has been provide by AOARD Project FA2386-12-4026.

References

1. M.J. Buckingham, E.M. Giddens (2006), On the acoustic field in Pekeris waveguide with attenuation in the bottom half space, *J. Acoust. Am.*, 119(1), 124-142.
2. M.D. Collins and M.F. Werby (1989), A parabolic equation model for scattering in the ocean, *J. Acoust. Am.* 85, 1895-1902.
3. R. D. Cook, D. S. Malkus, M. E. Plesha, and R.J. Witt (2004) *Concepts and Applications of Finite Element Analysis*, 4th Ed, John Wiley.
4. J.A. Fawcett (1997), Coupled-mode modeling of acoustic scattering from three-dimensional axisymmetric objects, *J. Acoust. Am.* 102, 3387-3393.
5. G. J. Fix, S.P. Marin (1978), Variation methods for underwater acoustic problems, *Journal of Computational Physics*, 28, 253-270.
6. G. V. Frisk (1994), *Ocean and Seabed Acoustics – A theory of Wave Propagation*, PTR Prentice Hall, New Jersey.
7. R.H. Hackman and G.S. Sammelmann (1986), Acoustic scattering in an inhomogeneous waveguide: Theory, *J. Acoust. Am.* 80, 1447-1458.
8. R.H. Hackman and G.S. Sammelmann (1988), Multiple-scattering analysis for a target in ocean acoustic, *J. Acoust. Am.* 84, 1813-1825.
9. F. Ingenito (1987), Scattering from an object in a stratified medium, *J. Acoust. Am.* 82, 2051-2059.
10. F.B. Jensen, A. Kuperman, M.B. Porter, H. Schmidt (2011), *Computational Ocean Acoustics*, 2nd Ed., Springer, New York.
11. M.C. Junger and D. Feit (1972), *Sound, Structures and their Interactions*, MIT Press, Cambridge.
12. L.E. Kinsler, A.R. Frey, A. B. Coppens, J.V. Sanders (2000), *Fundamentals of Acoustics*, 4th Ed., John Wiley & Sons, New York.
13. W. Luo and H. Schmidt (2009), Three-dimensional propagation and scattering around a conical seamount, *J. Acoust. Am.* 125, 52-65
14. N.C. Makris (1998), A spectral approach to 3-D object scattering in layered media applied to scattering from submerged spheres, *J. Acoust. Am.* 104, 2105-2113.
15. G.V. Norton and M.F. Werby (1991), A numerical technique to describe acoustical scattering and propagation from an object in waveguide, *J. Appl. Phys.* 70, 4101-4112.
16. C.L. Pekeris (1948), Theory of propagation of explosive sound in shallow water, *Memoirs of Geological Society of America*, 27, 1-116, 1948.
17. J.S. Perkins, W.A. Kuperman L.E. Tinker and G.T. Murphy (1992), Active matched field processing, *J. Acoust. Am.* 91, 2366.
18. M.B. Porter and E.L. Reiss (1984), A numerical method for computing ocean acoustic modes, *J. Acoust. Am.*, 76, 244-252.

19. M.B. Porter (2001), The KRAKEN normal mode program, SACLANT Undersea Research Center.
20. A.G. Sazontov, A.L. Matveyevand N.K. Vdovicheva (2002), Acoustic coherence in shallow water: Theory and observation, *IEEE Journal of Oceanic Engineering*, 27(3), 653-664.
21. H. Schmidt and J. Lee (1999), Physics of 3D scattering by rough surface and buried targets in shallow water, *J. Acoust. Am.* 105, 1605-1617.
22. H. G. Schneider (1977), Excess sound propagation loss in a stochastic environment (a), *J. Acoust. Am.*, 62(4), 871-87.
23. C.P. Vendhan, G.C. Diwan, S.K. Bhattacharyya (2010), Finite-element modeling of depth and range dependent acoustic propagation in oceanic waveguides, *J. Acoust. Am.*, 127, 3319-3326.
24. M. Zampolli, A. Tesei and F.B. Jensen (2007), A computationally efficient finite element model with perfectly matched layers applied to scattering from axially symmetric objects, *J. Acoust. Am.* 122, 1472-1485.
25. http://oalib.hlsresearch.com/Modes/AcousticsToolbox/

Publications

1. C. P. Vendhan (2013) Structural Analysis of Deep Water Offshore Structures – Part I, *Proceedings of the Institution of Engineers, Part M: Journal of Engineering for the Maritime Environment*, August 2013, Vol.227, pp. 226-232.
2. A.D. Chowdhury, C.P. Vendhan and S.K. Bhattacharyya (2015) Propagation of low frequency acoustic waves in a shallow water ocean over a semi-infinite solid seabed*, Indian Journal of Geo-Marine Sciences*, Vol 44, pp. 202-212.
3. S. Mudaliar, C.P. Vendhan, and C. Prabavathi (2016) Remote Sensing of the Ocean Environment using Finite Element Methods, in *Environmental Applications of Remote Sensing*, Intech Publications, pp. 197-234.
4. A.D. Chowdhury, C.P. Vendhan, S. Mudaliar and S.K. Bhattacharyya (2016) Study of a Rayleigh-Ritz approximation to depth eigenproblem of shallow water acoustic waveguides, *Journal of Sound and Vibration*, (under review).
5. Sunny Kumar, C.P. Vendhan and Krishnan Kutty (2016) Study of water wave diffraction around cylinders using a finite-element model of fully nonlinear potential flow theory, *Ships and Offshore Structures,* Vol 11, pp. 1-14.
6. Ravi Challa, S.C.Yim, V.G. Idichandy, C.P. Vendhan (2014) Rigid-object water-entry impact dynamics: finite-element/smoothed particle hydrodynamics modeling and experimental validation, *J. Offshore Mechanics & Arctic Engg*, Vol 136, pp 031102-1 to 031102-12.
7. S. Mudaliar, C.P. Vendhan, and C. Prabavathi (2016) A Rayleigh-Ritz approach to Green's function of an inhomogeneous layer, *USNC URSI Meeting*, Boulder CO, 4-7 Jan 2017.
8. A.D. Chowdhury, C.P. Vendhan and S.K. Bhattacharyya (2013) Low frequency acoustic wave propagation in shallow water ocean over semi-infinite solid sediment Layer, *International Conference and Exhibition on Underwater Acoustics*, Corfu, Greece, June 2013.
9. C.P. Vendhan , A.D. Chowdhury , S. Mudaliar, and S.K. Bhattacharyya (2014) Eigenproblem for an Ocean Acoustic Waveguide with Random Depth Dependent Sound Speed, *IEEE International Symposium on Antennas and Propagation and USNC-URSI Radio Science Meeting*, Memphis, TN, USA, July 2014.
10. S. Mudaliar, C.P. Vendhan, C. Prabavathi, and A.D. Chowdhury AD (2016) Radiation from axisymmetric bodies in depth dependent shallow water ocean, *IEEE Antennas and Propagation Society-URSI Joint Symposium*, Puerto Rico, 26 June – 1 July 2016.
11. A.D. Chowdhury, C.P. Vendhan, Deepak Kumar and S.K. Bhattacharyya (2013) Rayleigh-Ritz approximation of normal mode solution for depth dependent ocean waveguides, *National Workshop on Underwater Acoustics, Signal Processing & Communication*, PES, Bangalore, March 2013.

12. A.D. Chowdhury, C.P. Vendhan and S.K. Bhattacharyya (2015), Pressure field in depth dependent ocean acoustic waveguides using Rayleigh-Ritz approximation, *International Conference on Theoretical, Applied, Computational and Experimental Mechanics*, Indian Institute of Technology Kharagpur, India, December 2015.
13. A.D. Chowdhury (2016) *Studies in Computational Ocean Acoustics*, PhD Thesis (in preparation), IIT Madras.

Awards and Honours:

SAGE Award: '2013 SAGE Highly Commended Paper' award for his paper entitled "Analysis of Deepwater Offshore Structures: Issues and Challenges' published in the Special Issue on Structural Analysis of Deep Water Offshore Structures.

National Award in the field of Ocean Science and Technology for the year 2015 by the Ministry of Earth Sciences, Government of India.

Keynote Address "Hydrodynamics of Fluid-Structure Interaction" in MARHY 2016 *International Conference on Computational and Experimental Marine Hydrodynamics*.

Collaboration:

The entire project work was a collaboration between C.P. Vendhan of IIT Madras and S. Mudaliar of AFRL, Sensors Directorate. The proposal itself was based on discussions between the two during 2012. Since then there were periodic correspondences on the all technical aspects of the project. The IEEE International Antennas and Propagation Symposium in Memphis during July 2014 was an occasion when there were face-to-face research discussions between Vendhan and Mudaliar. Part of the work of the project was carried out as thesis work of IIT Madras student A.D. Chowdhury. A useful product of this work is the development of a simulation software package "Computational Ocean Acoustics Toolbox".